Delft University of Technology
Master of Science Thesis in Embedded Systems

Improving Ultrawide Band Ranging Using Two Antennas

Akhil Jain
Supervised by Dr. Mitra Nasri,
Kenneth Garvey,
Dr. Daniel Kornek

Improving Ultrawide Band Ranging Using Two Antennas

Master of Science Thesis in Embedded Systems

Embedded and Networked Systems Group
Faculty of Electrical Engineering, Mathematics and Computer Science
Delft University of Technology
Mekelweg 4, 2628 CD Delft, The Netherlands

Akhil Jain
Supervised by Dr. Mitra Nasri,
Kenneth Garvey,
Dr. Daniel Kornek
a.jain-2@student.tudelft.nl
akhil.jain@de.bosch.com

16/02/2021

Author
Akhil Jain (a.jain-2@student.tudelft.nl)
(akhil.jain@de.bosch.com)
Title
Improving Ultrawide Band Ranging Using Two Antennas
MSc Presentation Date
23/02/2021

Graduation Committee

Dr. Marco Zuniga	Delft University of Technology
Dr. Mitra Nasri	Eindhoven University of Technology
Dr. Alle-Jan van der Veen	Delft University of Technology

Abstract

Ultrawideband technology can be used to measure the distance between two device equipped with ultrawideband transceivers. Multiple ultrawideband devices known as anchors can localize a device that supports ultrawideband communication after each anchor measures the distance between itself and the device. The anchor and the tag can measure the distance between themselves by measuring the time of flight of the ultrawideband messages exchanged between them. If the location of the anchors are known, the location of the device can be computed. However, errors in range measurements can cause errors in localization of the device. There are many sources that can cause errors in the measured range between the anchor and the tag. For example, when the tag transmits a signal, and the path between the anchor and the tag is blocked, the signal may be attenuated to such an extent that it may go undetected at the anchor, causing the anchor to measure the time of arrival of a delayed reflection.

In this thesis, we aim to find a solution to improve the ranging accuracy when an anchor is equipped with two antennas. We target approaches that can be implemented on an embedded processor with limited resources. In order to improve the ranging accuracy, we first investigate various machine learning based classifiers that can identify non-line of sight and line of sight signals. Next, for each of the classified signal, we train and test various machine learning based regression models that will predict the true distance from the distance measured by the anchor. We conclude the thesis, by assessing the robustness of the derived classification and regression models by evaluating the range improvements in measurements taken in different scenarios.

Preface

This thesis report marks the end of my master studies in embedded systems with a specialization in software and networking at the Delft University of Technology. This research was conducted at Robert Bosch GmbH, in the Automotive electronics and body electronics campus in Germany, under the project Perfectly Keyless.

I would firstly like to extend my gratitude to my supervisor, Dr. Mitra Nasri, for bringing the best out of me. Her constant encouragement and support has helped me overcome roadblocks and bring out the researcher in me.

Secondly, I would like to thank my company supervisors, Kenneth Garvey and Daniel Kornek for giving me the opportunity and the resources to carry out this research.

I would also like to thank Michael Koeppl, Dominik Hub, Konstantin Hoffmann and Sergej Kerbel and Dietmar Eggert from Robert Bosch GmbH for providing me support with the hardware and the measurement setup on which I was able to record measurements.

Needless to say, I would also like to thank my friends in Netherlands, Kaustubh Agarwal, Teodor Nikolov and Paris Panagiotou who kept on supporting me mentally from their experiences in writing a thesis.

Akhil Jain

Delft, The Netherlands
16th February 2021

Contents

Acronyms

Acronyms	Actual name
AOA	Angle of Arrival
CAN	Control Area Network
CIR	Channel Impulse Response
GBM	Gradient boosting machine
LOS	Line of Sight
NLOS	Non-Line of sight
PDF	Probability Density Function
PDOA	Phase Difference of Arrival
RF	Random Forest
RMSE	Root Mean Square Error
SVM	Support Vector Machine
TOA	Time of Arrival
TOF	Time of Flight
TDOA	Time Difference of Arrival
UWB	Ultrawide Band

Table 1: **Abbreviations**

List of Tables

List of Figures

Chapter 1

Introduction

The approval of *ultrawide band* (UWB) technology in 2002 by the Federal Communication Council (FCC) [11] has triggered a wide range of research related to use cases of UWB. One of the widely used applications of UWB is ranging. Two devices embedded with UWB transceivers can accurately measure the *time of arrival* (TOA) of the received UWB signal and using that information calculate the distance between themselves. Multiple UWB devices known as anchors measure the distance between themselves and a device they are trying to locate. With prior knowledge of the location of the anchors and the range measurement derived by each anchor, the location of the device can be deduced.

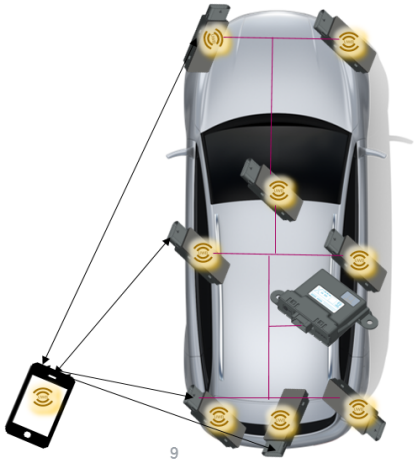

(a) **Anchors around the vehicle localizing with a tag**

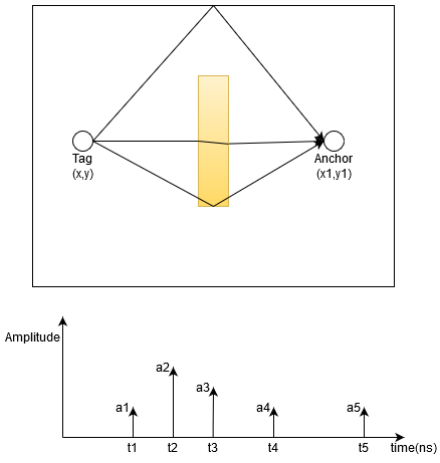

(b) **Multipath environment and the accumulated signals at the receiver**

Robert Bosch GmbH has been investigating the localization aspect of UWB, and its application in automotive under the *Perfectly Keyless* project. Anchors are installed with UWB transceivers and are placed at fixed known locations around the chassis of the vehicle as shown in figure 1.1a. Each anchor is connected to the master device via a *Control Area Network* (CAN) bus. The master has prior knowledge of the location of each anchor. When a UWB device comes in range with the vehicle, each anchor on the vehicle measures the range between

itself and the device which is sent to the master over the CAN bus. The master device extracts the range information from the CAN bus and estimates the location of the device.

The accuracy of localization depends on the accuracy of the range measurements reported by the anchors. However, due to inaccurate estimates of the TOA of the received signal, the range measurements reported by each anchor may have a ranging error that results in inaccurate localization of the device. One such reason is the orientation of the device antenna with respect to the anchor antenna. That is, the gain of the antenna is dependent of the polarization and the pattern of the antenna. Due to the non-existence of isotropic antennas, in this thesis, we investigate the performance of range improvement using two cross polarized antennas.

1.1 The Problem

In an ideal world, if all anchors provide an accurate estimation of the range, one can estimate the exact location of the device. However, like any other electromagnetic signal, UWB is prone to (i) interference and noise from background sources (when multiple users are using the same frequency at the same instant), (ii) Multipath interference when the signals reflect off surrounding objects causing multiple copies of the signal arriving at the receiver (iii) *Non-line of sight* (NLOS) issues when an obstacle blocks the direct line of sight path between the transmitter and receiver [15].

UWB devices can range with other devices by accurately measuring the TOA of the signal corresponding to the direct path. Depending on the environment, UWB waveform reflect from surrounding objects, that creates multiple copies of the transmitted signal, that arrive at the receiver with different delays and intensities as shown in figure 1.1b. The receiver then has to correctly identify and measure the TOA of the first received signal. This is because the direct path is the shortest distance a signal has to travel, hence, corresponds to the first peak received at the receiver. As shown in figure 1.1b, the signal corresponding to the straight line joining the tag and the anchor, is received first at time instant t_1. When there are no obstacles blocking or placed around the transmitter and receiver, the receiver receives a single copy of the signal which is identified as the first path. However, when an obstacle blocks the direct path between the transmitter and the receiver, the signal corresponding to the direct path may be attenuated that it may go unnoticed at the receiver. This may cause the receiver to measures the TOA of a time delayed multi-path signal, that results in a positive bias error in the final distance measurement. From figure 1.1b, the signal has to measure the time of the first arriving signal (t_1). But due to the attenuation offered by the blockage, the first arriving signal will be received with a low amplitude. This may cause the receiver to assume the signal to be a noise signal, and measure the timestamp of the second or third arriving signal at t_2 or t_3 respectively.

The intensity with which a signal is received at the receiver also depends on the orientation of the antenna. Hence, a signal arriving with a high energy may be significantly attenuated by the orientation of the receiving antenna. This may cause the signal to be attenuated at the receiver. The amount of

power extracted by the antenna depends on the difference in polarization of the antenna and the incoming signal [2].

1.2 Related Work

As discussed, range measured in a NLOS scenario have a high error associated with them which can lead to bad localization results. One method to avoid inaccurate localization due to errors in ranging is by knowing the anchors that have detected a NLOS scenario. This way, only the range measurement with low ranging error can be used for localizing the tag. Chen Huang [17] and Jiancun Fan [10] are among researchers that have developed machine learning based classification models that can identify the nature of a signal (LOS or NLOS). However, all these models and metrics were derived for a system with a single antenna.

Range measurements identified as LOS can be used for localization due to low ranging error, while errors for NLOS signals need to be mitigated before using it for localization due to the large positive bias error associated with them. Chen [25] and Li Cong [21] tried solving the problem of localization using statistical techniques however (i) their methods require the availability of range measurements from all anchors present, and (ii) at least three of these measurements should have a direct LOS. This can cause blackouts in our system if none of the anchors have a LOS path.

1.3 Solution Approach

In this thesis, we introduce techniques to improve the ranging accuracy when an anchor is equipped with two antennas positioned orthogonal to each other. We approach the problem by classifying signals as LOS or NLOS by training machine learning based classification models using input features extracted from two antennas. We compare our model with some of the state-of-the-art solutions based on the classification accuracy, input feature size and complexity. And then, for each class, we train a regression model to predict the true range from the measured range. We focus on investigating classification and regression models that have low complexity in terms of memory and runtime. For this thesis, we target to restrict the error in ranging to less than 30 cm.

1.4 Research Questions

In this thesis we try to answer two research questions.

- **RQ1**: *What is the impact of a second antenna on identifying NLOS signals using machine learning based classifiers?*
  With this question, we want to understand the effect of using features from a second antenna in identifying whether the signal is a LOS or an NLOS signal.
- **RQ2**: *How can machine learning based regression methods be used to improve the accuracy of ranging? What is the impact on ranging accuracy when two antennas are used?.*

By answering this question, we want to understand how well can regression based models be used to predict the true range measurements and the improvement in prediction when features are extracted from the second antenna.

1.5 Contributions

To answer RQ1, we

- evaluate the classification accuracy improvement when they are extracted from two antennas using the binary hypothesis theorem.
- evaluate the performance of different classification models on classifying LOS and NLOS signals when trained on the features extracted from two antennas.
- show the improvement in classification accuracy of some of the state-of-the-art classification models using features from two antennas.

For RQ2, we train regression models to predict the true distance for signals classified as LOS and NLOS. We compare the performance of different regression models for mitigating LOS and NLOS error based on the measured root mean squared error and the size of the model. The regression models are trained using features extracted from a (i) single antenna and (ii) two antennas to understand the impact of using a second antenna. We conclude our thesis by testing our classification and regression models on unseen data, that were collected when a second vehicle is parked next to the vehicle on which our anchor is placed.

1.6 Thesis Structure

Chapter 2 provides a brief introduction to the channel estimation parameters that are used to derive features for the classification and regression models. Chapter 3 introduces some of the state-of-the-art solutions. Chapter 4 provides an overview on the classification and regression models used, ranging accuracies measured in different scenarios. Chapter 5 elucidates the experiments that were conducted to answer the research questions. Lastly, chapter 6 concludes the thesis and chapter 7 lists down possible directions for future research.

Chapter 2

Background

2.1 Introduction

In this chapter, we first introduce the two way ranging method, that is used to calculate the *time of flight* (TOF), and consequently, the distance between the two UWB devices. Then we introduce the method of measuring the TOA used by our system and the available channel estimation parameters available that can be used to extract features.

2.2 Two way ranging

The distance between two devices can be estimated using the two way ranging protocol, that requires both the devices involved in ranging to measure the timestamp corresponding the transmission and reception of a signal within one ranging round. A ranging round is a series of messages exchanged, which at the end computes one distance measurement. The anchor and the tag run their own clocks, and no clock synchronization is required for this method. The ranging round starts with the tag sending a *poll* message followed by the anchor sending the response message, and ending by the tag sending the *final* message [8]. The anchor and the tag record the transmit and receive time for the *poll*, *response* and the *final* message as shown in figure 2.1.

At the end of the round, the tag sends the timestamp results to the anchor. These results are sent in the form of *tag round time* (T_{rnd}) and *tag reply time* (T_{rep}), that is computed as:

$$T_{rnd} = t_2^T - t_1^T \tag{2.1}$$

$$T_{rep} = t_3^T - t_2^T \tag{2.2}$$

The anchor computes the *anchor round time* (A_{rnd}) and the *anchor reply time* (A_{rep}) as:

$$A_{rep} = t_2^A - t_1^A \tag{2.3}$$

$$A_{rnd} = t_3^A - t_2^A \tag{2.4}$$

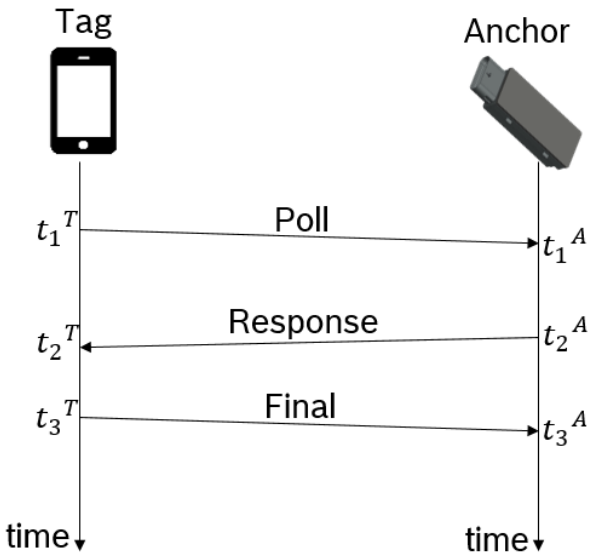

Figure 2.1: **Two way ranging**

T_{rnd}, T_{rep}, A_{rnd} and A_{rep} can be used to derive the TOF:

$$TOF = \frac{T_{rnd} * A_{rnd} - T_{rep} * A_{rep}}{T_{rnd} + A_{rnd} + T_{rep} + A_{rep}} \tag{2.5}$$

The distance between the two devices can be calculated my multiplying the TOF with the speed of light.

2.3 Timing Measurement

Section 2.2 talks about the ranging protocol that is used to measure the TOF by measuring the transmit and receive time of UWB signals. This section talks about the method for accumulating a timestamp for a received signal.

2.3.1 Channel Impulse Response

Radio signals are electromagnetic waves that propagate in different directions on leaving the antenna. These signals may interact with surrounding objects. Based on the object physical characteristics, these signals may be reflected or may pass through the object. Hitting the objects may also cause a phase shift in the colliding signals. Due to different distances travelled by the radio signal, these signals are received as delayed time signals at the receiver as shown in figure 1.1b. CIR is a measure of the intensity of the multipath component received by the receiver. It is the plot of the signal strength received over time.

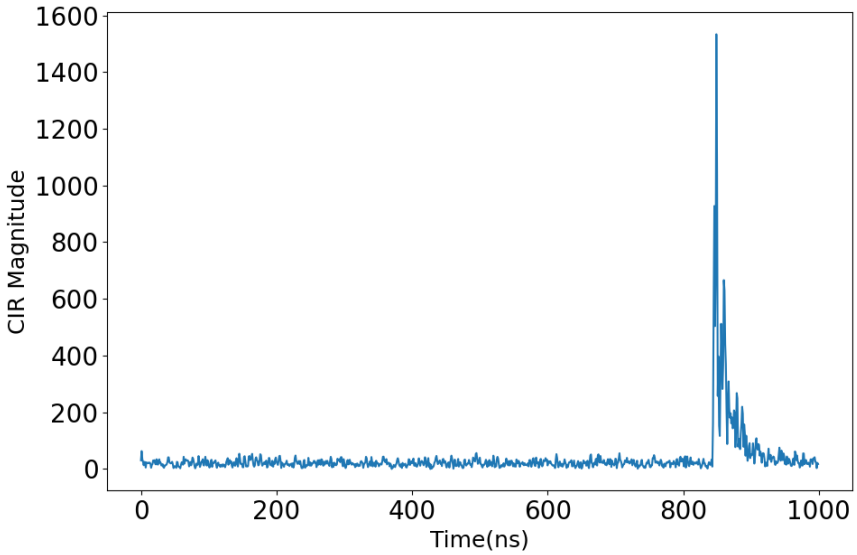

(a) **NLOS scenario**

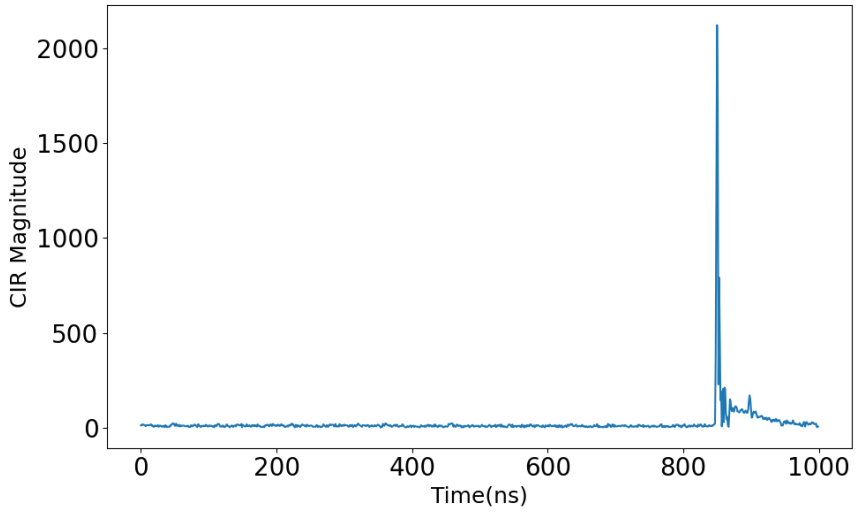

(b) **LOS scenario**

Figure 2.2: **Channel impulse response accumulated in (a) NLOS and (b) LOS scenario**

From [1], received CIR can be expressed as:

$$h(t) = \sum_{i=1}^{L} a_i \xi(t - \delta_i) \tag{2.6}$$

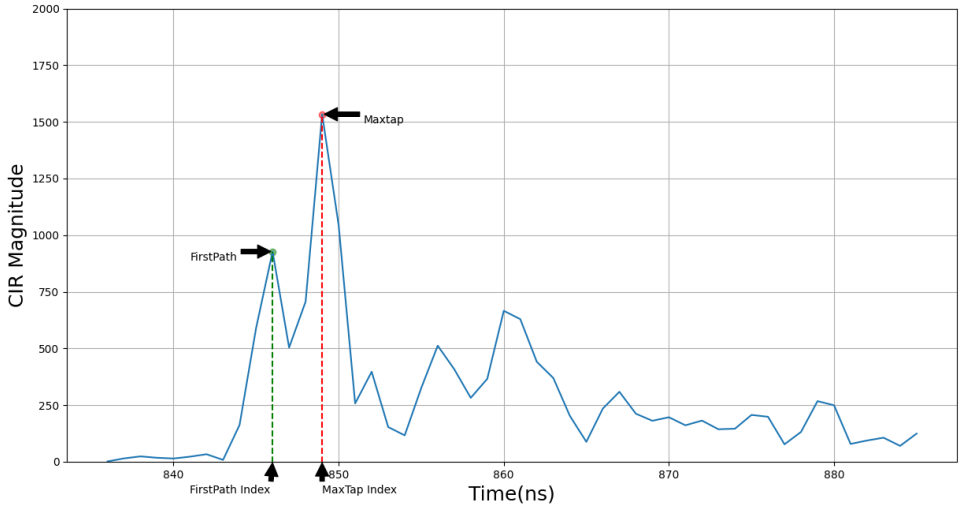

(a) **NLOS scenario**

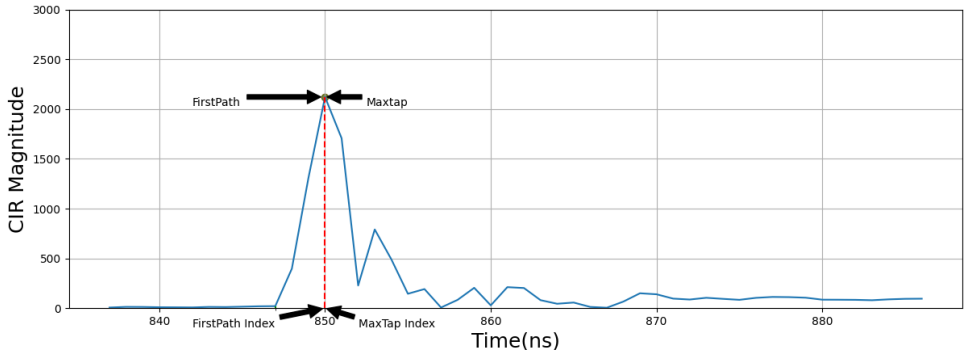

(b) **LOS scenario**

Figure 2.3: **CIR accumulated in LOS and NLOS scenario**

where a_i is the complex amplitude and δ_i is the time delay associated with a received signal. $\xi(.)$ is the pulse distortion function[1]. However, for this thesis, it is important to understand that h(t) denotes the series of signals arriving with different delays and different amplitudes. CIR plot accumulated in a NLOS scenario and LOS scenario is shown in figure 2.3a and 2.3b respectively. It can be seen that in a LOS scenario, there is a single peak of the highest magnitude, followed by reflections from the surroundings. In a NLOS scenario, one can identify multiple peaks in the CIR, indicating a large amount of reflections from surrounding obstacles.

2.3.2 Time of Arrival Estimation

A time of arrival algorithm on the UWB transceiver determines the signal corresponding to the first path from the received channel impulse response. The time of arrival of the detected first path signal is used to calculate the distance between the two devices. The accuracy of ranging is dependent on the performance of the TOA estimation algorithm. The TOA estimation on our system is

predefined and is taken as the leading peak. From figure 2.3b, the leading peak, which is also the highest peak is identified as the first path.

2.4 Channel Estimation

In our system, a *digital signal processor* (DSP) is responsible for accumulating the signal, plotting the CIR, performing the time of arrival estimation and returning the timestamp. When requested, the DSP can provide additional information regarding the received signal to the main processor. This information is used to form input features that will be used as inputs to the classification model. The channel estimation parameters available from the DSP are:

- **CIR**: The CIR is a result obtained after performing a cross correlation of a known preamble with the preamble of the received signal. The preamble is a terenary code that is present in the beginning of a UWB message. The raw CIR values for a received signal is captured and can be read by the application. A total of 1024 CIR values can be read from the DSP, and is available in a discrete format sampled at 1GHz. Each CIR sample occupies 4 bytes of memory (2 bytes of imaginary part and 2 bytes of real part). The DSP allows the main processor to limit the number of CIR values to read. Hence, we can read 50 CIR samples as shown in figure 2.3, and the CIR will occupy 200 bytes of memory in RAM.

- **Edge Index ($\tau_{edgeindex}$)**: The position on the CIR buffer, where the first threshold crossing of a signal was detected. The edge index helps to determine the starting index in the CIR buffer.

- **First Path Power ($\mathbf{P_{FP}}$):** The power of the multipath component signal that was detected as the first path signal by the time of arrival estimator. This value is available in raw form and can be linearly transformed to its decibel value.

- **Max Tap Power ($\mathbf{P_{Maxtap}}$):** The power of the multipath component corresponding to the maximum power of the accumulated signal. In a LOS scenario, the max tap power is the same as the first path power as shown in figure 2.3b. Although the CIR returns the raw values, the max tap power returns the power corresponding to the maximum raw value in the CIR. This value is available in raw form and can be linearly transformed to its decibel value.

- **First Path Index ($\tau_{firstpath}$):** The index on the CIR buffer where the time of arrival estimator estimated the signal as the first path. Figure 2.3b and 2.3a mark the first path index in the CIR.

- **Max Tap Index (τ_{maxtap}):** The position on the CIR, where the signal with the maximum amplitude was detected. As marked in figure 2.3, the first path index and max tap index coincide in a LOS scenario as the direct path signal arrives without attenuation at the receiver.

- **Noise Power ($\mathbf{P_{NoisePower}}$):** The noise floor power measured by the receiver.

- **Overall Power ($\mathbf{P_{Overall}}$):** The total power received by the receiver.

For the experiments, we only consider a 50 nanosecond window of the channel impulse response, staring from 10 nanoseconds before detected edge index. Figure 2.2 shows the entire CIR accumulated in a LOS and a NLOS scenario, and figure 2.3 plots the window that we use to extract the features for the classification model. The reason for doing this are two fold:

- We were able to capture the first path signal, and the max tap signal within this snapshot.
- No useful information was observed beyond the 50 nanosecond snapshot. This can be seen in figure 2.2.

Chapter 3

Related Work

In this chapter, we discuss the some of the research that has been conducted in order to identify NLOS signals and mitigate the error associated with them. In section 3.1, we discuss some of the statistical features that can be derived from the received signal that can classify LOS and NLOS signals. Some of these techniques are used to train machine learning based classification models to predict the scenario with higher accuracy. Different classification models and the features used are discussed in section 3.1.2. In section 3.2, we shed light on some of the NLOS error mitigation techniques that have been adopted. Finally, we show the extent of research that has been performed on dual antenna solutions in section 3.3 and conclude the related work in section 3.4.

3.1 Line of sight and non-line of sight identification

The need for identifying NLOS signal in performing localization stems from the high ranging error reported by these signals. This is due to the high attenuation offered by blocking obstacles, causing the direct path signal to go undetected at the receiver. Researchers have proposed TOA estimators [16] to accurately identify the first path signal from the received CIR. However, for this thesis, the TOA estimation is out of scope, as the digital signal processor performs the TOA estimation, which is company proprietary to the chip manufacturer.

3.1.1 Statistical Techniques

Based on the received UWB signal, different channel estimation parameters were derived that can be used to identify NLOS scenarios. Researchers have shown that channel information gathered while receiving the signal can be used to classify signals. Jie Zhang et.al [36] and Bruno et.al [29] showed that the kurtosis of the channel impulse response, Bo You et.al [33] showed that the ratio between the first path power and the overall power can be used to can be used to identify NLOS scenarios. Bruno et.al [29] also showed the performance the skewness of channel impulse response, difference between the total power and the first path power identify non-line-of-sight scenarios with high accuracy. Ali et.al [24] shows the use of root mean square delay and max spread delay in

Author	Metric
Jie Zhang[36]	Kurtosis of CIR
Bruno[29]	Skew of CIR
Ali[24]	Peak-to-lead-delay
Ali[24]	Root mean square delay
Ali[24]	Max spread delay
Bruno[29]	Power difference
Bo You[33]	Power Ratio

Table 3.1: **Statistical metrics based on channel parameters**

NLOS identification which is used as parameters to a gaussian mixture model in [10]. The contribution of researchers to identify NLOS signals is summarized in table 3.1. In this thesis, we extract some of these statistical features and use them as an input to our classification models.

3.1.2 Machine learning techniques

The last decade showed an increase in research on machine learning(ML) techniques to identify NLOS signals using features discussed in 3.1.1 as inputs to the classification model.
The effect of distance versus the *received signal strength* (RSS) follow a pathloss model in a LOS scenario, which changes when the LOS is blocked. Fabrizio et. al [5] and Valentin et.al [3] trained their models using a features extracted from a series of distance and the measured signal strength.
The CIR of the received signal was investigated in order to identify NLOS by Jeppe Bro Kristensen[19] using *support vector machine* and *linear discriminant analysis models* (LDA). Each nanosecond for the CIR was used as an individual input.
Chen Huang et.al [17] derived and compared three machine learning models(SVM, random forest and artificial neural networks) to identify NLOS scenarios. Chen and his team investigated angular features for identification and showed that it provided high error rates on all three models. The work of some other researchers that used classification models to identify NLOS scenarios is summarized in table3.2. All the above discussed classification models are trained on features extracted from a single antenna. In this thesis, we will investigate the classification performance with two antennas.

Although most of the research focuses on discarding NLOS range measurements due to high ranging error, it is possible for some NLOS signals to provide low error in its range measurement. Shing in [20] and Valentin in [3] performed classification with three classes, treating the NLOS with low error as the third class. As it will be discussed later in the thesis, we consider LOS and NLOS signals with low range error as the same class.

Data collected by researchers to train classification models lacked randomization. For example, in [17], LOS and NLOS data were collected after placing the antennas at fixed orientation on the top of the vehicle. In [5], data was collected at fixed locations distanced 0.5 meters apart, inside a building, while in [27], data was collected in an open area with no obstacles placed around the measurement setup. Bruno et.al [29] collected data in a factory environment,

Author	Model	Parameters
Fabrizio Carpi [5]	Threshold Detection	Kurtosis, skew, hyperskew mode of measured RSS
Valentin Barral [3]	Support Vector Machines	Mean of RSS and Distance
Jeppe Bro Kristensen [19]	Support Vector Machines	Channel Impulse Response
Jeppe Bro Kristensen [19]	Linear Discriminant Analysis	Channel Impulse Response
Chen Huang [17]	Support Vector Machine	Kurtosis, Skew, Rise time, Max power, root mean square delay, Rician K factor
Chen Huang [17]	Random Forrest	Kurtosis, Skew, Rise time, Max power, root mean square delay, Rician K factor
Jiancun Fan [10]	Gaussian Mixture Models	Mean spread delay, root mean squared delay, CIR taps crossing threshold
Weijie Li [32]	Support Vector Machines	Kurtosis, mean excess delay, maximum power, root mean square delay, Strongest Power, max amplitude, total energy, mean and variance of CIR
Reza Zandian [34]	Logistic regression	Peak Path Power,first path power, Skew, Kurtosis, Peak to lead delay, received signal strength, Power difference, signal-to-noise ratio
Zhuoqi Zeng [35]	Support Vector Machine	Maximum amplitude of CIR, rise time, mean excess delay, root mean square delay, Kurtosis, Skew

Table 3.2: **Work performed on machine-learning solutions for non-line-of-sight identification**

after placing the transmitter and receiver at fixed heights. For this thesis, the location and orientation of the device was varied to a high extent. Data was collected in the presence of human interference, device inside a backpack, and device held at varying heights.

3.2 Error mitigation

When a non-line-of-sight measurement is made, the localization system can either ignore its measurement or can perform mitigation techniques to correct the range measurement. Contrary to this belief, Lorenz [27] used artificial neural networks with channel estimation parameters as inputs to estimate the true distance in a line-of-sight environment. The need for error correction in LOS environments is due to under ranging(measured distance is lower than the true distance) which occurs because of TOA estimation error as stated in [32].

Most of the literature focuses on correcting localization measured by multiple anchors using maximum likelihood estimation[21] or measuring the residual of ranging error[25]. These methods generally involve taking all possible combination of anchors, 3 at a time, and measuring the residual in each combination. The final localization estimate is the anchor combination with the least residual. Regression methods on NLOS identified signals has not been performed. In this thesis, we use various regression models, namely random forest, gradient boosting and cubist for single as well two antennas to reduce the range error measured in NLOS scenarios. For the regression models, we use the input features used by [27].

3.3 Dual antenna solutions

Using multiple antennas can be beneficial, as the second antenna can provide a different perspective on the channel, that the first antenna may have missed. Based on the antenna configuration, one can expect different improvements.

- **Spatial Diversity**: In spatial diversity, multiple antennas are placed less than half a wavelength apart. Spatial diversity helps achieve angle of arrival estimation(AOA) where the angle of the incoming signal can be determined. This can be achieved using *phase difference of arrival* PDOA [9] (where the difference in the phase received between the two antennas) and *time difference of arrival* (TDOA) (Time difference of the signal arrival times at the two antenna) [14][18][30].

- **Polarization Diversity**: Polarization diversity can be achieved by placing the antenna poles orthogonal to each other. The need of polarization stems from the concept of antenna gain being proportional to the cosine of the difference between the transmitting and receiving antenna. Hence, LOS scenarios can report high ranging errors as the signal is highly attenuated by the antenna. The gain of using two antennas with cross polarization is shown in [28].
  Malik et. al [22] showed the use of polarization diversity with dual antenna can improve the *bit error rate* (BER) and the coverage area. He was also able to show insignificant improvement in coverage and BER using more than 2 antennas.

To the best of our research, ranging improvements with the use of two antennas has not been investigated. Since light cannot travel faster than its natural speed, selecting the least range measured by the two antennas as the final distance is shown in [7]. However, this may not be the best approach, due to the possibility of under range measurements reported by the receiver.

3.4 Conclusion

There is no study that considers dual antenna solutions for LOS and NLOS identification or for LOS and NLOS error mitigation. Our research will focus on investigating the influence of a second antenna on the classification accuracy of LOS and NLOS identification, and regression models to improve ranging accuracy for LOS and NLOS identified signals.

Chapter 4

System Design

4.1 Solution Overview

Figure 4.1 provides an overview of the chapter. We first discuss the method of accumulating data, and the scenarios we have considered. In section 4.3, we describe how channel estimation parameters gathered in section 4.2 can be used to extract features which are then used to train our model to identify LOS and NLOS signals in section 4.4. Regression models are trained and tested on signals identified as LOS as well as signals identified as NLOS (Section 4.5).

4.2 Data accumulation

4.2.1 Dataset

In order to train and test the classification models, channel estimation parameters labelled LOS and NLOS were collected in three scenarios: (i) open garage (figure 4.2a), (ii) second vehicle parked on the right of the vehicle (figure 4.2b) (iii) second vehicle parked in front of the vehicle (figure 4.2b). Data accumulated from scenario (i) is used to train the classification and regression model, while data accumulated from scenario (ii) and (iii) are used to test the robustness of the trained models. LOS labelled data was collected by performing a random walk around the vehicle, such that there is no obstacle between the direct path

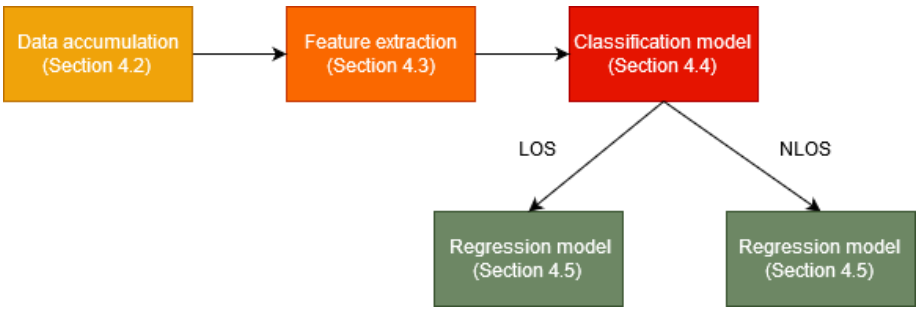

Figure 4.1: **Solution overview**

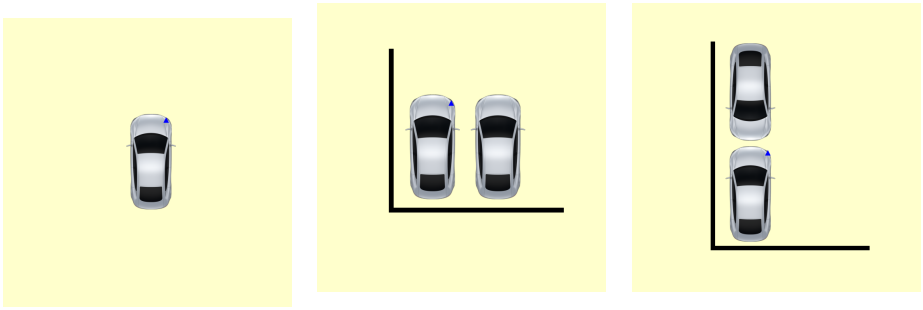

(a) **Open Garage**

(b) **Scenario 1 configuration**

(c) **Scenario 2 configuration**

Figure 4.2: **Three scenarios in which data was collected (a)open garage (b)two vehicle parked next to each other (c)two vehicles parked in front of each other**

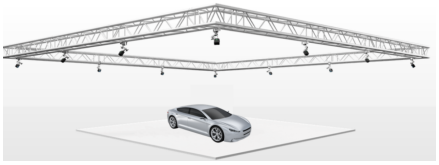

(a) **Motion capture setup with vehicle**

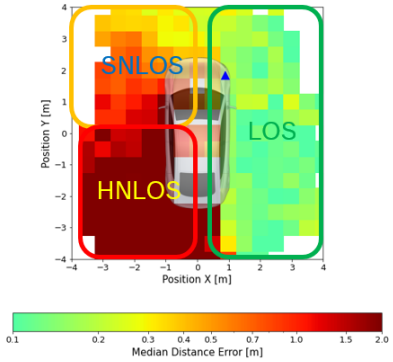

(b) **Median error reported by the system**

Figure 4.3: **System setup**

between the transmitter and receiver. NLOS data is collected after performing a random walk around the vehicle, such that there is no direct path between the anchor and the tag. It was ensured that the data collected is exhaustive: The device was kept at different orientation, and heights.

In order to validate the need to classify signals as LOS and NLOS, data was collected in an open garage after placing the anchor on the front bumper as shown in figure 4.3b. The ground truth measurements were accumulated by the motion capture system, that uses *infrared* cameras positioned at fixed locations around the vehicle to calculate the position of objects installed with IR reflectors with millimetre level accuracy. This system allowed us to collect data in an exhaustive approach. The anchor and the tag were installed with infrared reflectors, which enabled the motion capture system to record the accurate location of the two devices. The sub micrometer accuracy of the motion capture system helped us gain very accurate ground truth range measurements. A conceptual representation of our setup is shown in figure 4.3a.

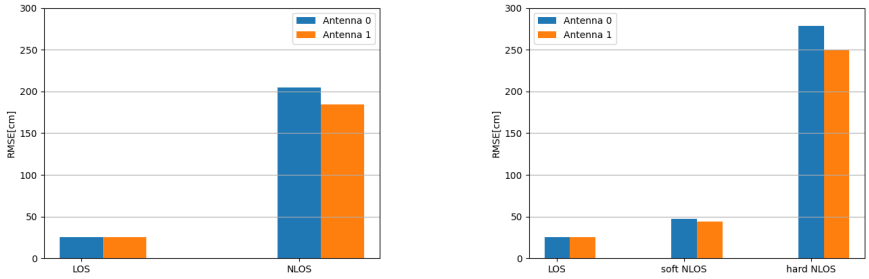

(a) **Range error reported by the two antennas in LOS and NLOS scenerio**

(b) **Range error when NLOS is divided into *soft* NLOS and *hard* NLOS**

Figure 4.4: **Ranging error in (a) LOS and NLOS, (b) LOS, soft NLOS and hard NLOS scenarios**

The ranging error calculated using the *root mean square error* (RMSE) measured by the two antennas in LOS and NLOS scenarios is plotted in figure 4.4a. It is evident from the plot that LOS scenario report much lower errors than that reported in NLOS scenario. Hence, in the perspective of localization, the system can ignore anchor range measurements that are identified as NLOS by the anchor due to large positive bias error. This can prevent localization errors, by eliminating the the presence of NLOS range measurements in the final localization calculation.
From figure 4.3b, y coordinate greater than 0 and x coordinate less than 0 reported lower error compared to the left of the trunk, that reported ranging error greater than 2 meters, even though there is no direct LOS path between the anchor and tag in that region. This is probably because of the nature of the obstruction. Signals originating from these regions are able to arrive at the anchor with sufficient energy to be detected, as the obstructions does not attenuate the signals to a huge extent. Hence, based on this observation, NLOS signals can be further classified as *soft NLOS* and *hard NLOS* based on the nature of obstruction. In this thesis, we create three classes of data:

- **LOS**: Data was collected such that there were no obstructions between the direct path joining the transmitter and receiver antenna
- **Soft NLOS**: Soft NLOS data were collected in the region reporting a median error of less than 1 m and greater than 0.3 m as shown in figure 4.3b. Soft NLOS was also collected in LOS scenarios, with a human blocking the path between than anchor and the tag.
- **Hard NLOS**: Hard NLOS data was collected in regions reporting a median error greater than 1 m as shown in figure 4.3b. The entire body of the vehicle blocks the path between the anchor and tag, hence attenuating the direct path signal.

The corresponding RMSE error in table 4.4b. We can see an increase in the measured RMSE for the range measurement in hard NLOS scenario after removing the soft NLOS labelled range measurements. The RMSE error reported

by soft NLOS region is closer to the errors reported in the LOS region than to the errors reported from the hard NLOS region.

4.3 Feature Extraction

In this section, we discuss the features we used, and their extraction from the channel estimation parameters (Section 2.4). These features are used to train the classification model to identify LOS and NLOS signals.

Kurtosis[29] (K): The kurtosis is a statistical measure that gives an indication of how well the distribution resembles a Gaussian distribution. It gives an indication of the peakness of the distribution.

$$K = \frac{E[(|h(t)| - \mu_{|h(t)|})^4]}{E[(|h(t)| - \mu_{|h(t)|})^2]^2} = \frac{E[(|h(t)| - \mu_{|h(t)|})^4]}{\sigma^4_{|h(t)|}} \tag{4.1}$$

where h(t) is the CIR as described in equation 2.6, and $\mu_{|h(t)|}$ and $\sigma_{|h(t)|}$ is the mean and standard deviation of the amplitudes of the CIR.

Skewness[29] (S): The skewness is a statistical measure that gives an indication of the asymmetry of the distrubution.

$$S = \frac{E[(|h(t)| - \mu_{|h(t)|})^3]}{E[(|h(t)| - \mu_{|h(t)|})^2]^{1.5}} = \frac{E[(|h(t)| - \mu_{|h(t)|})^3]}{\sigma^3_{|h(t)|}} \tag{4.2}$$

where $\mu_{|h(t)|}$ and $\sigma_{|h(t)|}$ is the mean and standard deviation of the amplitudes of the CIR.

Mean Excess delay[24] ($\tau_{\mathbf{med}}$) The max delay spread provides an indication of the multipath richness of the CIR.

$$\tau_{med} = \frac{\int_{-\infty}^{\infty} t * |h(t)|^2 \, dt}{\int_{-\infty}^{\infty} |h(t)|^2 \, dt} \tag{4.3}$$

where h(t) is the accumulated channel impulse response, at time t.

Power Difference[29] ($\mathbf{P_{Diff}}$): The power difference can be estimated as the difference between the total power received by the antenna, and the power of the signal identified as the first path by the TOA estimation algorithm.

$$P_{Dif} = P_{Overall} - P_{FP} \tag{4.4}$$

Power Ratio[29] ($\mathbf{P_{Ratio}}$) : The power ratio is the ratio of the received first path power to the total power received. In a LOS scenario, with no obstacles, it is expected that the first path power approaches the total power, hence the power ratio approaches 1.

$$P_{Ratio} = \frac{P_{FP}}{P_{Overall}} \tag{4.5}$$

Peak to lead Delay[29] (PLD) The peak to lead delay is defined as the time difference between the first multipath component and the strongest multipath component. For a LOS scenario, the PLD should be close to 0 compared to a non line of sight scenario.

$$PLD = \tau_{maxtap} - \tau_{edgeindex} \tag{4.6}$$

MaxCIR[23]: The max CIR is the maximum amplitude of the CIR. The index of the CIR with the maximum amplitude can be indexed on the CIR buffer using the max tap index (τ_{MaxTap}).

$$maxCIR = max(|h(t)|) \tag{4.7}$$

where h(t) is the CIR (equation 2.6).

Count of energy taps[10](N_p) The number of signals on the CIR whose energy exceeded 85% of the total energy received. The energy of the signal can be expressed as[23] :

$$\epsilon_r = \sum_{i=1}^{L} |h(t)|^2 \tag{4.8}$$

4.3.1 Feature Performance

Probability density function (PDF) of the features discussed in section 4.3 is plotted in figure 4.5. As it can be seen for all the features, there is a clear difference in the distribution for data collected in LOS and NLOS scenarios. This proves the ability of these features to identify LOS and NLOS signals.

4.3.2 Feature Sets

In order to evaluate the performance of the classification model, we train different models with different sets of features, which are generated using the 7 out of the 8 features plotted in figure 4.5. We divide the features into sets based on their computation complexity:

- **Set0**: Training a model with Set0 will utilize all the eight features as inputs to the model.
- **Set1**: Training a model with Set1 will utilize the features that can be extracted only by parsing through the CIR. That is, these features have a computation complexity of at least O(n), where n is the size of the CIR window under consideration. Kurtosis, skewness and the max delay spread fall under set1.
- **Set2**: Set2 contains features that can be derived without parsing through the CIR. That is, these features have O(1) computation complexity. Power ratio, power difference and peak to lead delay and maxCIR fall under Set2.
- **Set3**: Set3 is the combination of the best performing features from Set1 and Set2. The classification performance of different features is discussed in section5.2.

A summary of all the feature sets is provided in table 4.1. While forming an input feature set for a classification model with two antennas, individual feature sets from the two antennas are concatenated to form a set which is used as an input to the classification model. N_P feature showed less than 70% (section 5.2) classification accuracy because of which, it is not used in any of the feature sets.

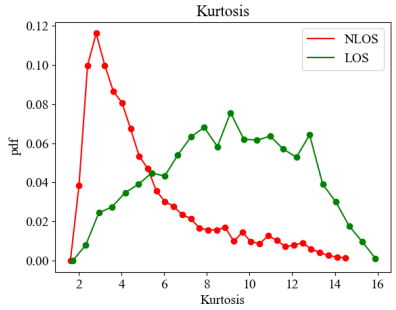

(a) **Kurtosis**

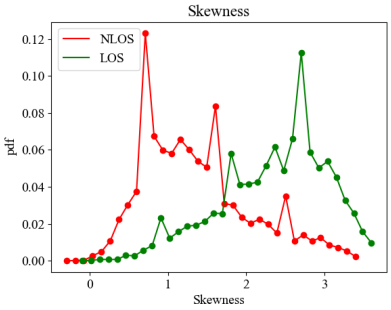

(b) **Skewness**

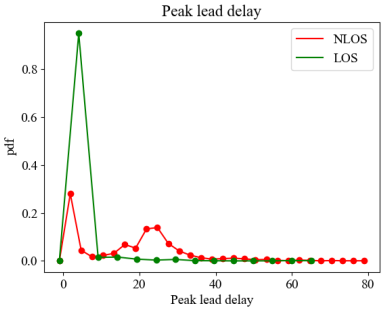

(c) **Peak-lead-delay**

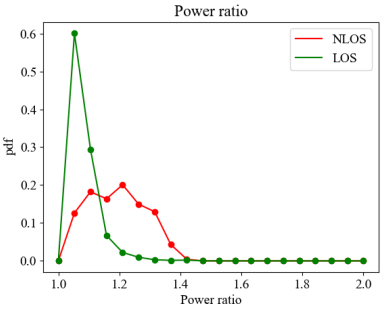

(d) **Power ratio**

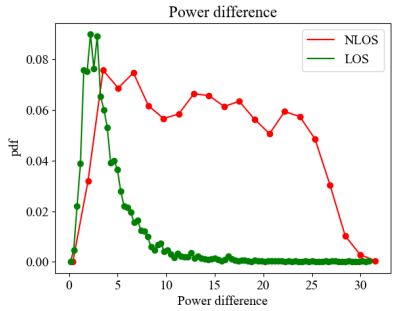

(e) **Power difference**

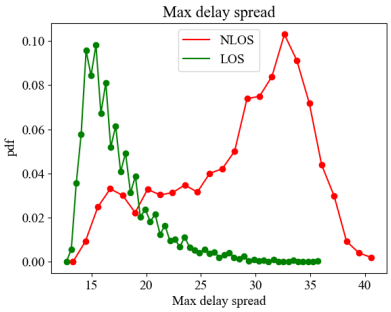

(f) **Max delay spread**

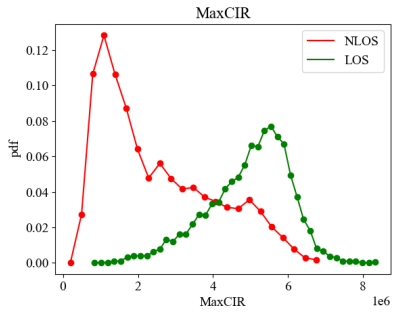

(g) **Max CIR**

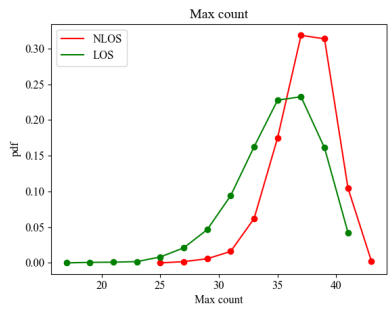

(h) **Max Count**

Figure 4.5: **Probability density function of all features in LOS and NLOS scenerios**

Set	K	S	P_{Diff}	P_{Ratio}	PLD	τ_{med}	Max CIR
Set 0	✓	✓	✓	✓	✓	✓	✓
Set 1	✓	✓				✓	
Set 2			✓	✓	✓		✓
Set 3			✓			✓	✓

Table 4.1: **Feature sets**

Model	nickname
Support Vector Machines [6]	*SVM*
Decision Tree [31]	*decision tree*
Random Forest [4]	*RF classifier*
Gradient boosting [13]	*GBM classifier*
AdaBoost [12]	*adaboost classifier*

Table 4.2: **Classification Algorithms**

4.4 Classification Model

In terms of machine learning, classification models aim at defining a model that relates a set of input features to a discrete output. A collection of input dataset, and the known outcome, is used to derive a function (or a model) that can predict the outcome. In classification models, the model predicts a discrete outcome. Data containing the features (as inputs) and the outcome (as output) is used to train the model. Since our first research question aims in predicting whether a given signal is a LOS or a NLOS signal, classification algorithms are used to make predictions given the accumulated features as inputs. For this thesis, we consider five classification algorithms. We choose these algorithms keeping in mind that the final model will be implemented on a processor with limited resources. The model is evaluated based on the classification accuracy,

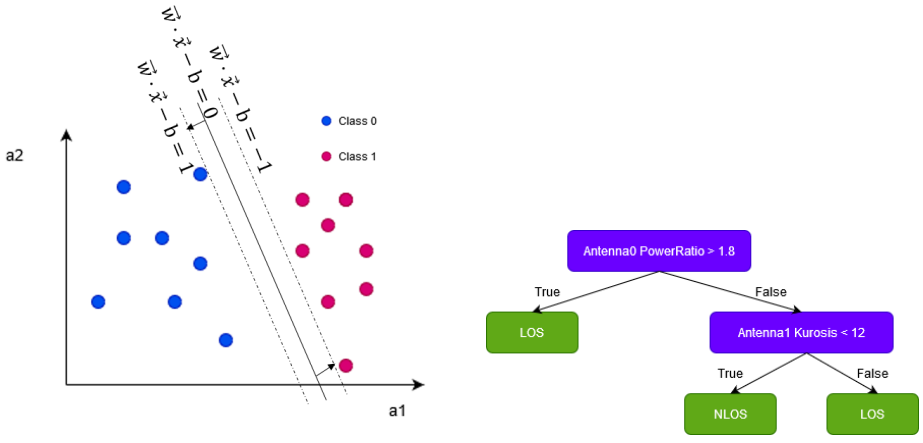

(a) **Support Vector machine** (b) **Decision Tree**

Figure 4.6: **Classification and Regression Models**

which is a ratio of the correct prediction by the total number of predictions. If we have two classes positive and negative, the overall accuracy of the model is calculated as:

$$Accuracy = \frac{TP + TN}{TP + FP + TN + FN} \tag{4.9}$$

where TP and TN are the number of times the model predicted a positive signal and a negative signal accurately, while FP and FN are the number of times the model predicted a positive signal to be negative and vice verse.

Support Vector Machine: The *svm* classifier models a linear or polynomial equation of a hyper plane that best separates two classes of data in N dimensions, where N is the number of input features to the model. The class of any input data is determined by the sign of the output when the input features are plugged into the hyperplane equation. An example for a *svm* classifier is given in figure 4.6a. Since the example plot has two features, the hyperplane is a line in two dimensions.

$$PredictedOutcome = \begin{cases} \overrightarrow{w} * \overrightarrow{x} - b < 0, & \text{class 0 identified} \\ \overrightarrow{w} * \overrightarrow{x} - b > 0, & \text{class 1 identified} \end{cases}$$

where $\overrightarrow{w}$ are the weights, $\overrightarrow{x}$ is the input feature vector and b is constant.

Decision Trees: A decision tree is formed by a series of conditional nodes and terminating leaf nodes that finally define the class of the test data. The feature space is broken down into decision nodes, until a terminating condition is reached. Decision trees are prone to over fitting and do not perform well when treated with a large feature set. An example of a decision tree is given in figure 4.6b. For an incoming signal, the P_{Ratio} value measured by the first antenna is compared in the first decision node. If the value is greater than 1.8, the signal is labelled as a LOS signal. If the P_{Ratio} value is less than 1.8, the kurtosis of the CIR accumulated by the second antenna is checked. If the kurtosis is greater than 12, the signal is labelled as LOS, else the signal is labelled as a NLOS signal.

Random Forest: Random forrest is an ensemble based classification model, where multiple decision trees are formed by training them on subsets of the input data and features. Each decision tree makes a prediction on an input dataset, and the class of the input signal is class with the highest number of predictions by the decision trees.

Gradient Boosting Classifier: Gradient boosting classifier is a tree based classification model, that builds trees based on weak learners from the previously formed trees. An initial decision tree is formed, and the next tree is trained on the wrongly predicted dataset by the first decision tree. Unlike random forest, each tree has unequal say in the final decision of the model.

Adaboost Classifier: Adaboost classifier is a boosting based ensemble classifier that generates multiple weak learners called stumps that are decision trees with depth as 1. Each stump is assigned a weight. The final outcome decision is taken place via voting, however, each stump has a vote corresponding to the assigned weight.

Binary Hypothesis test: The classification accuracy for individual features is evaluated using the binary hypothesis test [24][29]. Given two hypotheses:

H_1: Signal is LOS
H_2: Signal is NLOS

we can determine the scenario as LOS or NLOS by evaluating:

$$\frac{P(F|H_1)}{P(F|H_2)} \underset{H_1}{\overset{H_2}{\lessgtr}} 1, \tag{4.10}$$

where F represents individual features.
In order to determine the conditional probability $P(F|H_i)$, we approximate the probability distribution function for each feature in LOS and NLOS to follow a normal distribution. That is, from figure 4.5, we determine the mean and variance of each feature in LOS and NLOS.

$$P(F|H_1) = N(\mu_1, \sigma_1^2) \tag{4.11}$$

and

$$P(F|H_2) = N(\mu_2, \sigma_2^2) \tag{4.12}$$

where μ_1, μ_2 are the means and σ_1, σ_2 are the variance for the probability density function for LOS and NLOS scenarios for feature F respectively.
The binary hypothesis theorem, when extended for multiple inputs as:

$$\frac{P(f_0, f_1|H_1)}{P(f_0, f_1|H_2)} \underset{H_1}{\overset{H_2}{\lessgtr}} 1 \tag{4.13}$$

where f_0 and f_1 are the feature extracted from antenna 0 and antenna 1 respectively. This can be simplified if the features are considered to be independent variables, and hence

$$P(f_0, f_1|H_i) = P(f_0|H_i) * P(f_1|H_i) \tag{4.14}$$

where H_i are the initial hypotheses.

4.5 Regression Model

Regression models aims at predicting the relation between a set of input features and a continuous outcome. We use regression models to predict the true distance, using the measured distances by the antennas and some of the channel estimation parameters as inputs to the model. We predict the accuracy of the model by measuring the relative error:

$$RelativeError[\%] = \frac{y^{true} - y^{measured}}{y^{measured}} * 100 \tag{4.15}$$

where y_{true} is the true distance measurement and $y_{measured}$ is the model predicted range. The relative error is measured for each range measurement and is

Model	nickname
Random Forrest regressor [4]	*RF regressor*
Gradient boosting regressor [13]	*GBM regressor*
cubist regression [26]	*cubist regressor*

Table 4.3: **Regression Algorithms**

shown in the form of box plots. The overall ranging accuracy is evaluated using the root mean squared error expressed as:

$$RMSE = \sqrt{\frac{\sum_{i=0}^{N}(y_i^{measured} - y_i^{true})^2}{N}} \tag{4.16}$$

Where N is the number of measurements, and $y_i^{measured}$ is the model predicted range and y_i^{true} is the true range measurement for the i^{th} measurement.

We train and test three regression models on data identified as LOS and NLOS. The three regression models are different in their approach at generating the model. Random forest is a bagging based ensemble method, gradient boosting is a boosting based ensemble technique, and cubist generates applies a linear function at every leaf of the tree.

Random Forest Regression: Similar to random forest classifier, the final decision of a random forest regressor is the average of outcome from individual trees. The leaf nodes are continuous values.

Gradient Boosting Regression: Similar to the gradient boosting classifier, the output is the weighted average of the prediction from individual trees. Just like gradient boosting classifiers, decision trees for gradient boosting regressor is trained on the wrong predictions of previous decision trees.

Cubist: Cubist model generates a set of rules, and at the end of each rule, a linear equation as a function of the input feature is used to reduce the cost function for regression.

Chapter 5

Experiments and Results

This chapter elucidates the experiments conducted and results obtained for the classification and regression models. We begin our investigation by evaluating the performance of some of the commonly used features in identifying whether the signal is a LOS or a NLOS signal. In order to do this, we use the binary hypothesis test (section 5.2). These features are used as inputs to the machine learning based classifiers for predicting the nature of the signal (LOS or NLOS) with a higher accuracy (Section 5.3).

Once we have classified LOS and NLOS signals, we aim to reduce the ranging error of the classified signals. In order to do this, we use machine learning based regression models (section 5.4) that will predict the true range from the measured range. We will develop two regression models, one will be used for LOS identified signals, and the second will be used for NLOS identified signals.

Lastly, in section 5.5, we show the performance of our classifier (from section 5.3) and regression models (from section 5.4) in reducing the range error in various parking scenarios. In this chapter, we refer to all the classifiers and regression models using their abbreviations listed in table 4.2 and table 4.3 respectively.

5.1 Experimental Setup

All measurements were taken on an anchor housing two UWB silicons and two antennas. The silicon and antenna on the anchor identical, except for the fact that the two antenna orientation are orthogonal to each other. Figure 5.1 shows the two antennas placed 90 degrees to each other on the anchor. All decisions that will be made on selecting models are on the overall performance(accuracy) and the model size but not on the basis of the number of antennas used.

As discussed in section 4.2, we were able to identify a region around the vehicle that although being NLOS, reported range measurements with low range error. We evaluate the similarity of soft NLOS with LOS or hard NLOS by creating three datasets. For Dataset 1, soft NLOS signals and hard NLOS signals belong to the same class. This methodology has been used by most of the researchers. Classification for Dataset 3 is a 3 class classification problem, wherein, soft NLOS signals are treated as a different class. This approach was adapted by Shing in [20] and Valentin in [3]. In Dataset 2, soft NLOS signals are treated

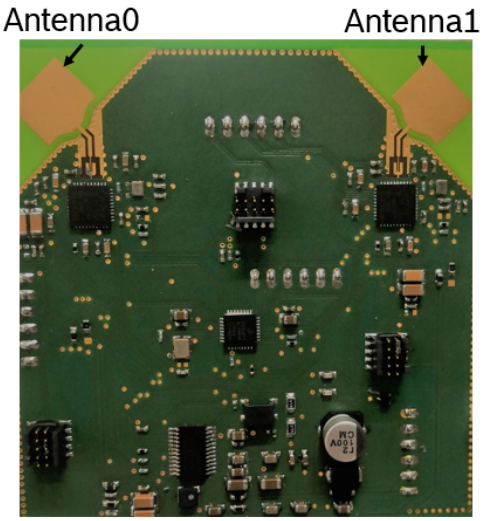

Figure 5.1: **Anchor hardware marking the two antennas used**

as LOS signals. A summary of the Dataset and the splits into different classes is tabulated in table 5.1.

We use the features evaluated in section 5.2 to train and evaluate the performance of 5 classification models namely SVM, decision tree , RF classifier, GBM classifier, adaboost classifier. All classification models are dependent on their hyperparameters. For each model, the hyperparameters were calculated using a grid search approach, where all the parameters are varied, and 5 fold cross validation is performed. In 5 fold cross validation, the Dataset is divided into 5 subsets (without repetition), 4 of which are used to train the model, and the accuracy is evaluated on the 5th subset. In the next iteration, the another of the 5 subsets becomes the testing data, while the other 4 subsets are used to train the model. This continues 5 times, until all the subsets was treated as a testing dataset. The hyperparameter configuration that provides the highest 5 fold mean accuracy is plotted along with the 95% confidence interval of the 5 fold cross validation accuracy.

Signals classified as LOS and NLOS are corrected after using regression models to predict the true range given the measured ranges and the channel estimation parameters as inputs. The same method of hyperparameter tuning is used to predict the best parameter configuration for regression models. Firstly, the dataset is split into a 80:20 ratio, where 80% forms the training data, while 20% data is the test data, on which the RMSE and relative error is plotted. In order to tune the hyperparameters, 5 fold cross validation is performed on the training dataset, and the model parameter configuration with the highest cross validation mean score is taken as the final model, and the RMSE and relative error is plotted for the selected model.

Our classification and regression models are concatenated and evaluated on data collected from two parking scenarios discussed in section 4.2. We evaluate the range error in the form of RMSE and the relative error of the received signals before classification, after classification and after applying the regression model to show the robustness of our solution.

Dataset	Scenario	Class 1	Class 2	Class 3
Dataset 1	LOS	4000	0	0
	Soft NLOS	0	2000	0
	Hard NLOS	0	2000	0
Dataset 2	LOS	2000	0	0
	Soft NLOS	2000	0	0
	Hard NLOS	0	4000	0
Dataset 3	LOS	3000	0	0
	Soft NLOS	0	3000	0
	Hard NLOS	0	0	3000

Table 5.1: **Dataset formulation for classification problem**

5.2 Feature evaluation

5.2.1 Introduction

In this section we evaluate the performance for some of the state-of-the-art features that were discussed in section 4.3 on single and dual antennas. We test the accuracy on classifying signals based on three datasets shown in table 5.1. From this experiment, we want to answer the following questions:

- What is the effect of adding a second antenna to the anchor?

The classification for each feature is performed using the binary hypothesis theorem discussed in section 4.4. For testing the classification accuracy from two antennas, the same feature is extracted from both the antennas. For example, to test the classification accuracy of PLD using two antennas for Dataset1, PLD for either class is extracted from both antennas, and the normalized PDF is calculated. The binary hypothesis theorem uses the normalized PDF for LOS and NLOS from both classes as discussed in equation 4.13.

5.2.2 Impact of Second antenna

Figure 5.2 shows the classification accuracy of each feature on the three datasets when two antennas are used. From the plots, it can be deduced the for all three datasets, the classification accuracy increased when two features from two antennas are extracted.

5.2.3 Feature Comparison

MaxCIR recorded the highest classification accuracy among the rest of the features on Dataset2 and Dataset3, while τ_{med} feature performed the best on Dataset1. Maxcount (N_p) reported the least classification accuracy as compared to the rest of the features. As shown in figure 5.3, the N_P feature has an accuracy of a low 60% as compared to the rest of the features that have a classification accuracy around 80% for Dataset1 and Dataset2. For this reason, N_p is not used as a dataset.

Author	Model
Jeppe Bro Kristensen[19]	Support Vector Machines
Jeppe Bro Kristensen[19]	Linear Discriminant Analysis
Chen Huang[17]	Support Vector Machine
Chen Huang[17]	Random Forrest
Weijie Li[32]	Support Vector Machines

Table 5.2: **State of the art solutions for comparisons**

5.2.4 Dataset Comparison

Figure 5.3 compares the performance of features from two antennas on the three datasets considered. All features report higher classification accuracy as compared to Dataset 1 and Dataset3. Moreover, Dataset 3 reported the lowest classification accuracy. For any future classification performance evaluation, we train our models on Dataset2.

5.3 Binary Classification

5.3.1 Introduction

In this section, we will train and evaluate different binary classification models using the features that were evaluated in section5.2 as inputs to different binary classification models and evaluate their accuracy on our system. We use Dataset 2 to train our models. As presented earlier, the features can classify Dataset 2 with the highest accuracy. Moreover, the N_P feature is not used to train the model due to the low classification accuracy as discussed earlier. From this experiment, we want to:

- Evaluate the performance of different classification algorithms with using different feature sets as inputs from the two antennas.
- Compare our classification models against the state-of-the-art solutions.

We first divide the list of features into 4 feature sets as shown in table 4.1. Since each antenna can form their own feature set, we perform a grid search approach, where different feature sets from both antennas are concatenated and used to train different classification models tabulated in table 4.2.

We then compare two of our best models against some of the state of the art solutions. The best models are evaluated based on the classification accuracy, feature extraction complexity and the model size (number of trees, and depth of trees).

5.3.2 Results

5.3.3 Evaluating Feature sets

Figure 5.6a-(e) show the accuracy obtained when using features from two antennas to train SVM, decision tree, RF classifier, GBM classifier and adaboost classifier models respectively. For all classification models, Set1 from antenna 0 and antenna 1 reported the lowest accuracy. The reason for this can be traced

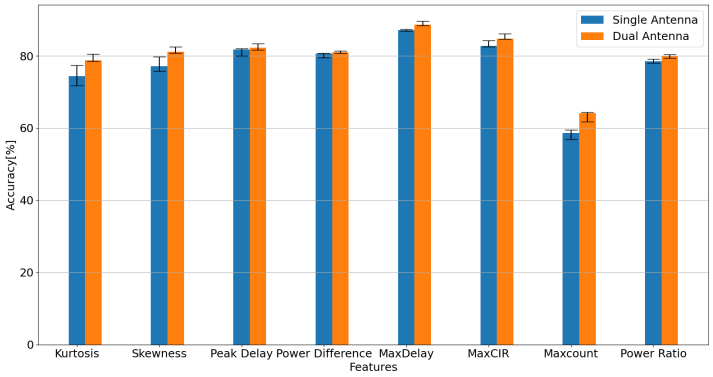

(a) **Dataset1: Single vs dual antenna classification accuracy**

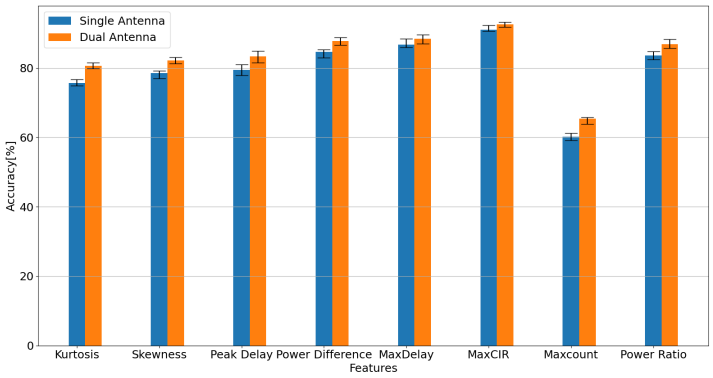

(b) **Dataset2: Single vs dual antenna classification accuracy**

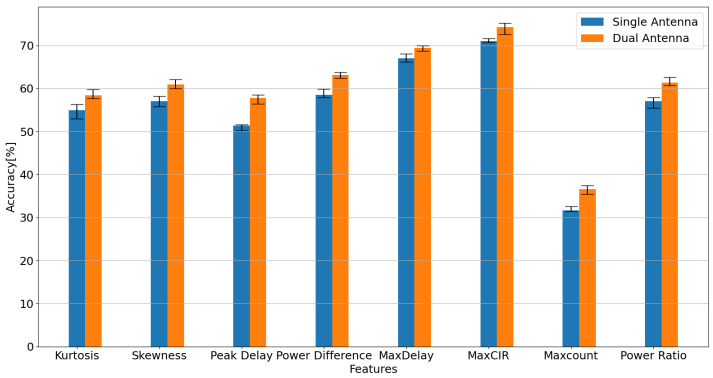

(c) **Dataset3: Single vs dual antenna classification accuracy**

Figure 5.2: **Accuracy comparison for single and dual antenna solutions for different datasets**

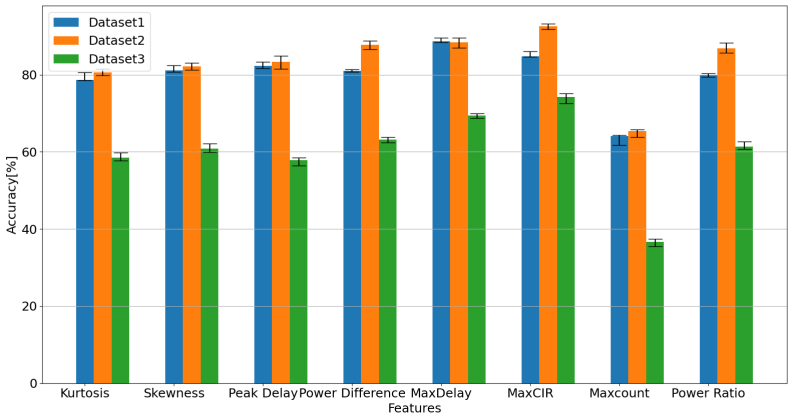

Figure 5.3: **Classification accuracy of different datasets with 2 antennas**

back to the classification accuracy of K and S feature, which was the lowest as compared to the rest of the features. Feature Set0 from both the antennas report the highest accuracy for all classifiers except for decision tree classifier. This may be because decision tree classifier does not perform well with increasing number of features, and Set0 use all features extracted from both antennas.

5.3.4 Narrowing Selection

All model configurations, except for configurations using feature Set1 from either antennas, are able to classify LOS and NLOS signals with an accuracy greater than 90%. In order to narrow down our search, we select the models based on the complexity of feature extraction. As discussed in section 4.3.2, feature Set2 contains features that have O(1) computation complexity. We focus on the 5 classification models, using feature Set2 configuration from both antennas. Features from Set2 can be computed directly from the received channel estimation parameters with the use of simple mathematical operations.

5.3.5 Model Selection

The 5 models using Set2 configurations are compared based on their classification accuracy and the model size. The model size is compared based on the number of trees used and the maximum depth of trees for tree based classifiers, and is considered 0 for non-tree based classifiers (like SVM classifier). Figure 5.5a and 5.5b plots the classification accuracy and the model size obtained for different classification models using feature Set2. Rf classifier has the highest accuracy but also has the largest model size. On the other hand, decision tree reported the lowest classification accuracy and the lowest model size for a tree based model. SVM and adaboost classifier models are able to classify with similar accuracy, however, SVM is a linear function, while adaboost classifier requires 36 trees to classify. GBM classifier has similar accuracy as compared to RF classifier and requires only 14 estimators to classify a signal.

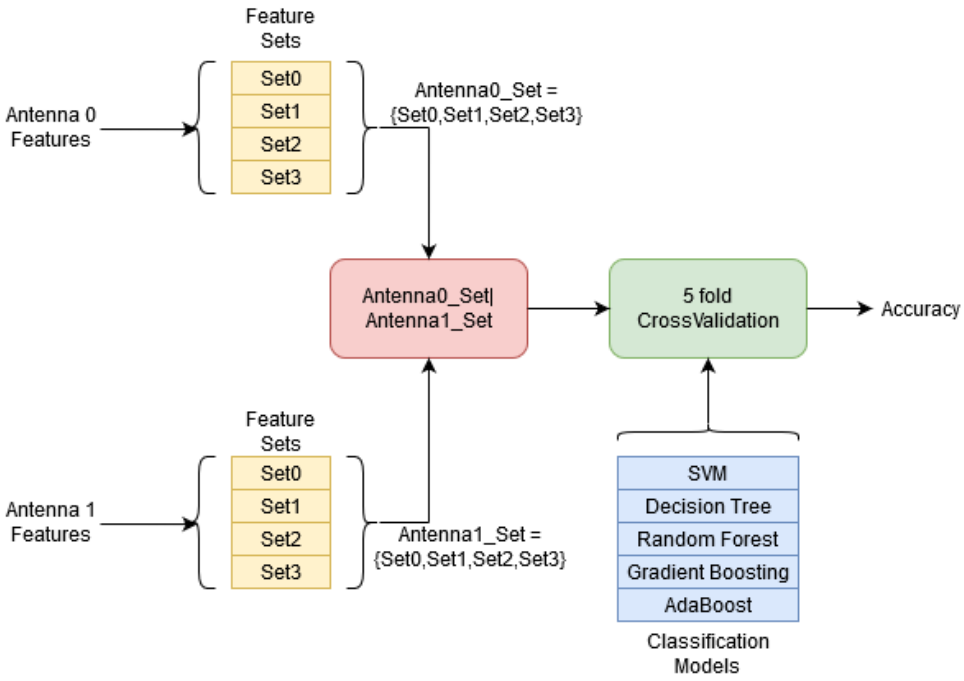

Figure 5.4: **Approach to evaluate classification accuracy**

5.3.6 Concluding Model Selection

Based on our observation, we will use GBM classifier for its high classification accuracy and small model size, and SVM classifier for to its simple implementation for further investigation. We will compare the two models against some of the state-of-the-art solutions, and will discuss the overall system performance in robust scenarios.

5.3.7 State of the Art Solutions

The two classifiers, namely SVM and GBM classifier trained with features from feature Set2 is compared with some of the state-of-the-art solutions tabulated in table 5.2. The state of the art solutions is trained on Dataset 2 from table 5.1. Although the state-of-the-art solutions were implemented on a single antenna, our extension of the these solutions to two antennas show an improvement over the single antenna implementation.

Accuracy : Figure 5.7a compares the accuracy of some of the state of the art classification models with our solution. Weijie's solution showed the greatest improvement when the second antenna is used. Jeppe Bro's solution to use SVM and LDA classifier with the accumulated CIR as inputs reported the highest accuracy. Our dual antenna GBM classifier model performs has similar accuracy to Chen Huangs random forest solution. However, GBM classifier has a much smaller model size as compared to the random forest solution by Chen Huang, as shown in figure 5.7b.

Feature size: Figure 5.7c compares the feature size of some of the state of the art classification models with our solution. Chen Huang's classifier from [17]

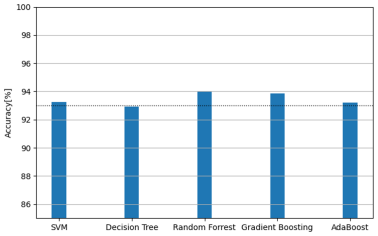

(a) **Classification accuracy for Set2 configuration**

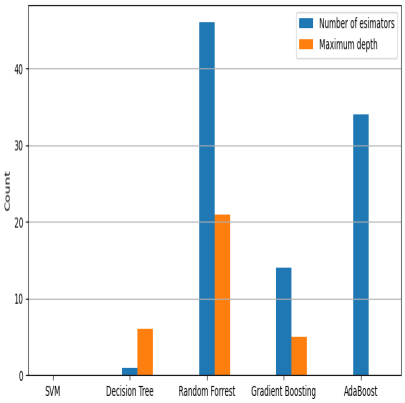

(b) **Number of trees and depth of trees**

Figure 5.5: **Set2 accuracy and model size**

uses 6 features as inputs to a SVM and RF classifier, 5 of which have O(n) computation complexity, while Jeppe in [19] uses individual CIR values(accumulated every nanosecond) as inputs to a SVM and a *(Linear Discriminant Analysis)* (LDA) classifier. Weijie Li in [32], uses 8 features, 7 of which have O(n) computation complexity. The two classification models discussed in this thesis uses 4 features having O(1) complexity from each antenna.

5.4 Range Prediction Using Regression

Regression models are used to predict the true range for signals identified as LOS and NLOS. Although a LOS signal has a low range measurement error, the classifiers classify soft NLOS and LOS signals as the same class, hence increasing the overall ranging error for the signals identified as LOS. For the regression based approach, we use the estimated channel parameters as inputs to the regression model. This is because, unlike classification models, we did not observe any relation between the channel estimation parameters except for the measured distance as shown in figure 5.8. The input to the regression models used to predict the true range are: (i) Measured distance (ii) Power of the signal identified as the first path ($P_{FirstPath}$), (iii) Noise power measured by the receiver ($P_{NoisePower}$) (iv) and the overall power ($P_{OverallPower}$).

We first discuss the use of regression models if a signal is identified as LOS. Since signals identified as LOS has a high range error due to soft NLOS signals, we will also investigate improving the range measurements for LOS identified signals. We then expand our investigation to NLOS signals, that produces high positive bias in its range measurements. For all the models, we use the same set of input features.

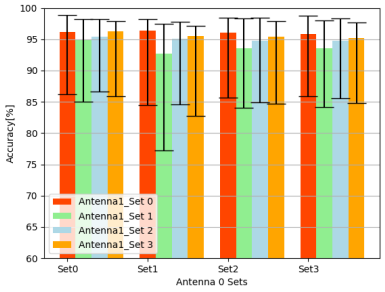

(a) **Support Vector Machine**

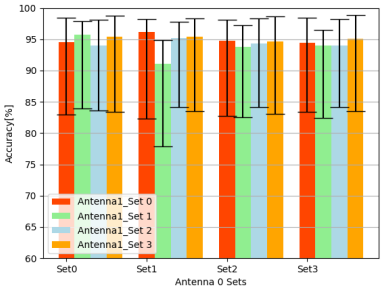

(b) **Decision Tree**

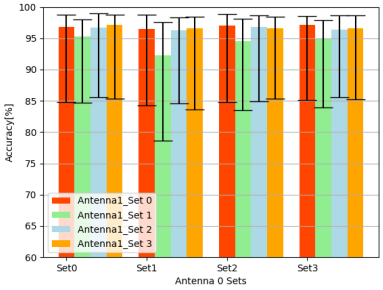

(c) **Random Forrest**

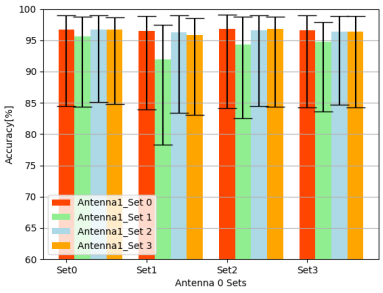

(d) **Gradient Boosting**

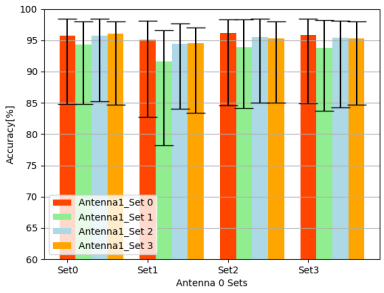

(e) **adaboost classifier**

Figure 5.6: **Accuracy comparison for different classification algorithms with dual antennas by varying feature sets**

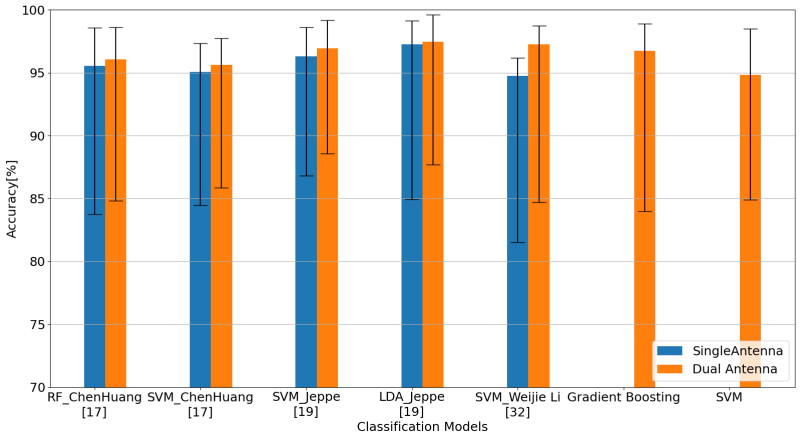

(a) **Accuracy comparisons with the state of the art**

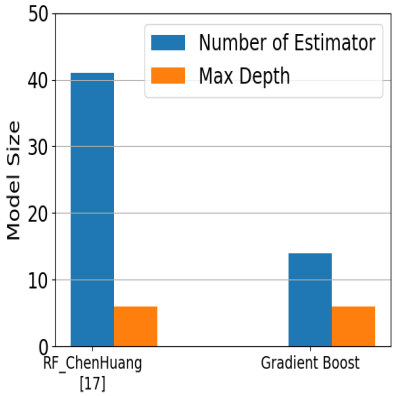

(b) **Model size comparisons with the state of the art**

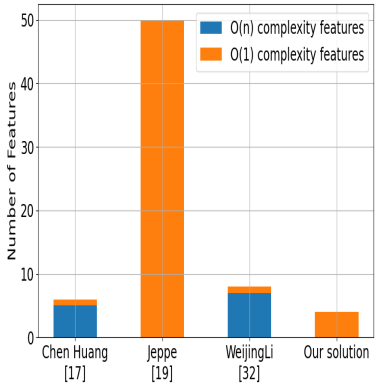

(c) **Feature size comparison**

Figure 5.7: **Accuracy and model size comparison with state of the art solutions**

5.4.1 LOS Error Mitigation

Figure 5.9a and 5.9c show the relative error when regression models are trained on features extracted from antenna 0 and antenna 1 respectively, and figure 5.9e shows the relative error when regression models are trained on features extracted from both antennas. Lastly, figure 5.9g compares the RMSE for antenna 0 and antenna 1 before and after regression models are applied. All three regression models (models trained on data from single and dual antennas) were able to reduce the measured RMSE from 38 cm in antenna 0 and 36cm in antenna 1 to less than 25cm. It can be observed that dual antenna regression models reported a lower RMSE than single antenna regression models. From the box plots, it is observed that the cubist reported the least minimum-maximum interval of ranging error (within 40%) among the three regression models and the lowest

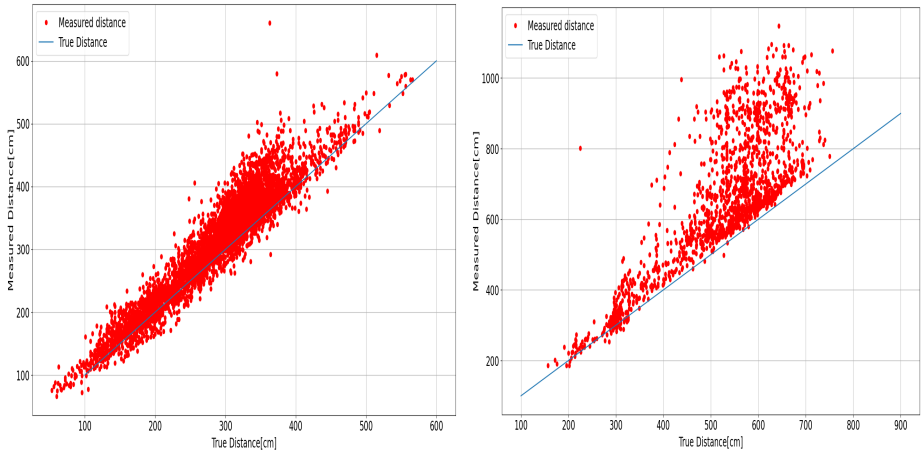

(a) **LOS and soft NLOS** (b) **Hard NLOS**

Figure 5.8: **True Distance vs Measured Distance for LOS and NLOS signals**

measured RMSE of 21.2cm when two antennas are used. GBM regressor reported the highest percentage of outliers, while cubist model reported the least for the dual antenna solution.

5.4.2 LOS regression model size

Figure 5.10a plots the number of estimators and the maximum depth of estimators for each regression model and configuration. Dual antenna configuration for cubist trees require only 4 rules(depth of 2), as compared to 5 rules(depth of 3) required by cubist model trained on features from a single antennas. It was observed that the correlation between the input feature and the outcome impacts the number of rules required. This correlation coefficient is returned whenever the cubist model is trained. The high correlation coefficient reported during cubist regression is probably because of the individual range measurements from both antennas report low errors and the measured range is close to the true range. On the other hand, RF regressor and gradient boosting regression models require 46 trees and 41 trees respectively when two antennas are used to train the model.

5.4.3 NLOS Error Mitigation

Figure 5.10b plots the number of estimators and the maximum depth of estimators for each regression model and configuration. Figure 5.9b and 5.9d show the relative error when regression models are trained on features extracted from a antenna 0 and antenna 1 respectively, and figure 5.9f show the relative error when regression models are trained on features extracted from both antennas. Lastly, figure 5.9h compares the RMSE for antenna 0 and antenna 1 before and after regression models are applied. All three regression models were able to reduce the RMSE by at least 78%, using a single antenna, while combined antenna configuration reported an approximate reduction by 79.8% . Antenna

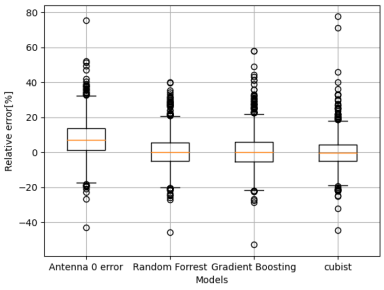

(a) **LOS with antenna0**

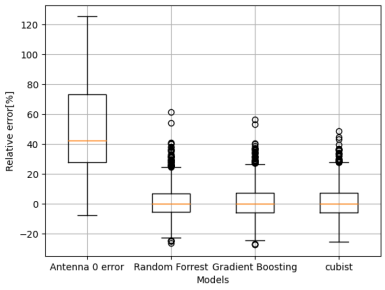

(b) **NLOS with antenna0**

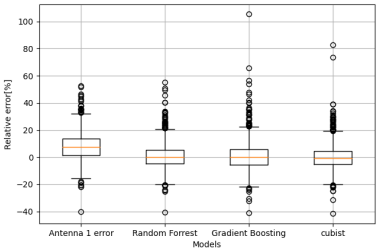

(c) **LOS with antenna1**

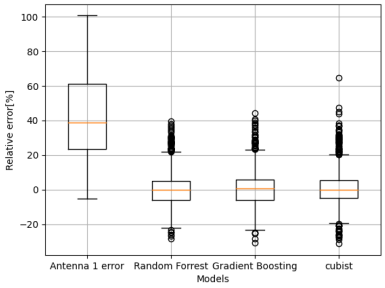

(d) **NLOS with antenna1**

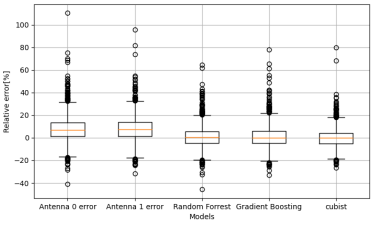

(e) **LOS with both antennas**

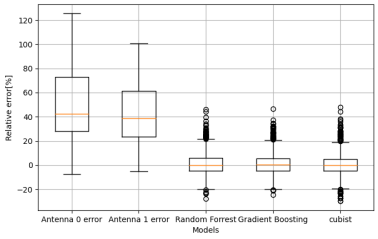

(f) **NLOS both antennas**

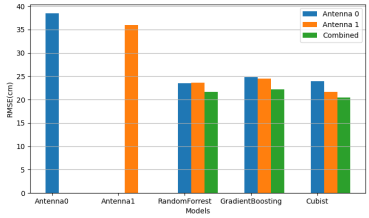

(g) **RMSE plot for LOS signals**

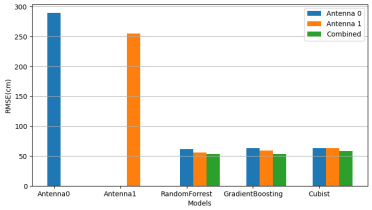

(h) **RMSE plot for NLOS signals**

Figure 5.9: **Relative error and RMSE plots for LOS and NLOS signals**

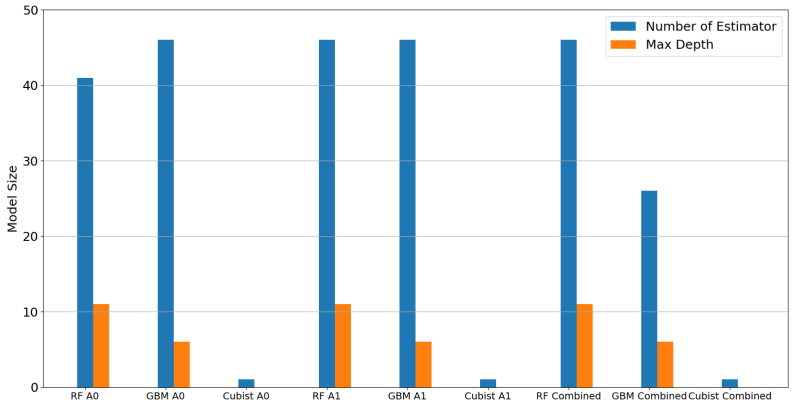

(a) **Model sizes for regression models in LOS scenarios**

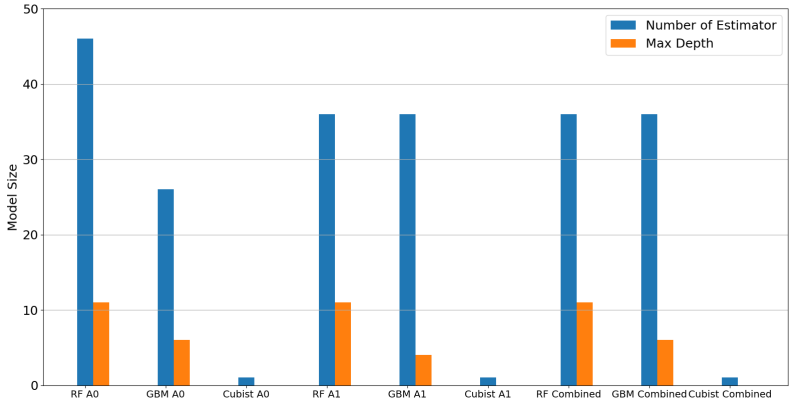

(b) **Model sizes for regression models in NLOS scenarios**

Figure 5.10: **Model size comparison for RF, GBM, cubist regression models using single and two antennas**

1 configuration for cubist, RF regressor, GBM regressor had approximately the same variance intervals, while antenna 0 showed high variance in the measured relative error than antenna 1.

5.4.4 NLOS Regression Model Size

The cubist regression model trained on features from antenna 1 used 14 rules, and when inputs from both antennas were used, the model used 35 rules to predict the true range. RF regressor and GBM regressor required 46 and 16 estimators respectively when antenna 1 is used, and 36 and 46 estimators when combined antenna configuration is used.

5.4.5 Conclusion

Cubist regression model trained on features from two antennas reported the smallest model size and the lowest RMSE among the rest of the regression models for LOS signals. For NLOS signals, all models reported similar RMSE, however, cubist regressor model trained on antenna 1 reported the smallest model size of only 14 rules.

5.5 Assessing Robustness

Once we have our trained classification and regression models, we validate our models by assessing the robustness. We have trained and tested the classification and regression models on data collected in an open garrage with no vehicles parked around the system under test. Our solution should not fail in a real world environment, where multiple vehicles are parked.

Data is collected from 2 different scenarios as discussed in section 4.2.1. For each of the two scenarios, 2000 points from LOS and 2000 points from NLOS were collected. The NLOS labelled data is an uneven mixture of soft and hard NLOS data. We use the SVM and GBM classifiers to classify signals as LOS and NLOS. Next, two regression models for predicting range measurements are used: (i) cubist regression trained with features from two antennas on LOS and soft NLOS data is used to predict the range for LOS identified signals (ii) cubist regression model trained with features from antenna 1 on hard NLOS data is used to predict the range measurements for NLOS identified signals. For both the scenarios, we test the performance of both the classifiers along with the cubist regression model. The RMSE and relative error is measured in the following three steps:

- Before the signals are passed to the classifier. This way, we know the true range error of the LOS and NLOS signals.
- After classification: Since NLOS signals are a mixture of soft and hard NLOS signals, there should be a rise in the measured RMSE for LOS and NLOS identified data from the true LOS and NLOS data, since soft NLOS signals with higher ranging error than LOS range measurements are classified as LOS.
- After regression: The RMSE and relative error is remeasured on the regression model predicted distances for LOS and NLOS classified signals. We expect the RMSE of the predicted range after regression should be less than the RMSE measured before and after classification.

5.5.1 Scenario 1

Figure 5.11a, 5.11b, 5.11c, 5.11d show the measured RMSE before classification, after prediction and after regression is applied on LOS and NLOS identified signals using SVM and GBM classifier classifier respectively in scenario 1. Figure 5.12a and 5.12b compares the measured RMSE for the three cases for LOS and NLOS signals. When GBM classifier is used, we can observe a 48% reduction in RMSE for NLOS identified signals and a 17% reduction in RMSE for LOS

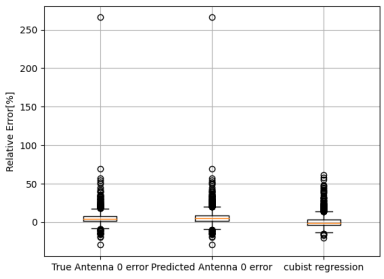

(a) **SVM classifier in LOS scenario 1**

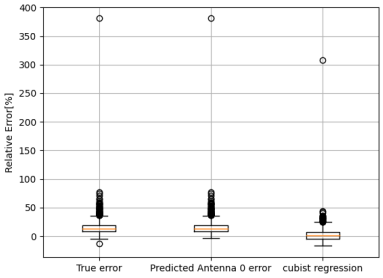

(b) **SVM classifier in NLOS scenario 1**

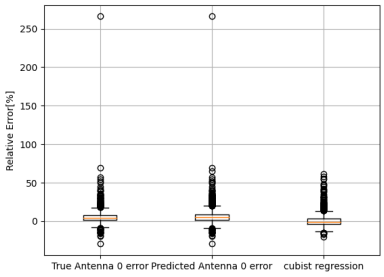

(c) **Gradient boost classifier in LOS scenario 1**

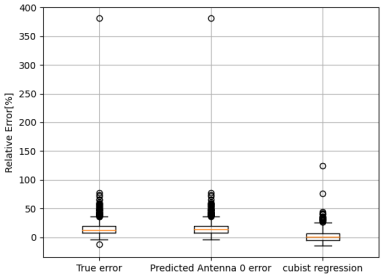

(d) **Gradient boost classifier in NLOS scenario 1**

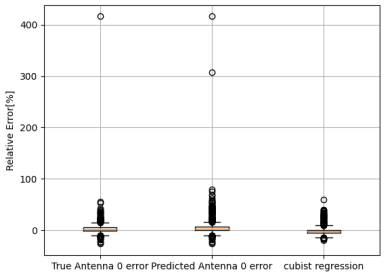

(e) **SVM classifier in LOS scenario 2**

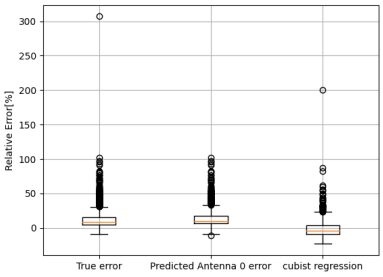

(f) **SVM classifier in NLOS scenario 2**

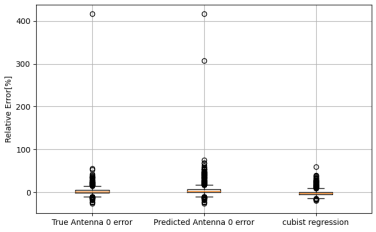

(g) **Gbm classifier in LOS scenario 2**

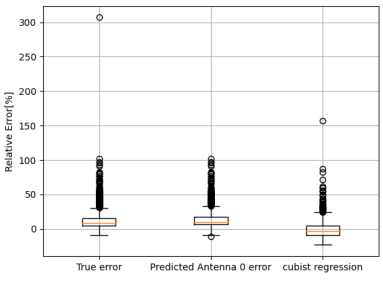

(h) **Gbm classifier in NLOS scenario 2**

Figure 5.11: **Box plot of relative error measured before classification on LOS and NLOS signals, after classification on SVM and gbm classifiers and after range prediction using cubist**

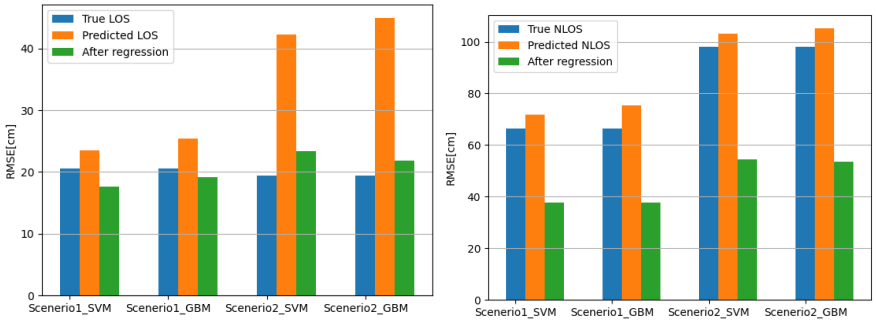

(a) **LOS classified signals** (b) **NLOS classified signals**

Figure 5.12: **RMSE plots LOS and NLOS signals before prediction, after prediction and after applying regression when a signal is identified as (a)LOS or (b)NLOS, in scenario 1 and scenario 2**

identified signals as compared to 50.9% reduction in RMSE for NLOS identified signals and 17.4% reduction on LOS identified signals when a SVM classifier is used. The both classifiers and regression models were able to limit the RMSE for LOS identified signals to less than 30 cm but NLOS identified signals still reported errors greater than 30cm.

5.5.2 Scenario 2

Figure 5.11e ,5.11f ,5.11g ,5.11h shows the measured RMSE before classification , after prediction and and after regression is applied on LOS and NLOS identified signals using SVM and GBM classifier classifier respectively. Figure 5.12a and 5.12b compares the measured RMSE for the three cases for LOS and NLOS signals. From the RMSE plots, there is a significant rise in the RMSE for the classified LOS signals from the true RMSE of LOS signals, for both classifiers. However, there is a small increase in the classified NLOS RMSE from the RMSE of the true NLOS signal. This indicates the possibility of NLOS signals, with high range error being classified as a LOS signal. From the box plots for true LOS signal, there is one outlier signal that has a relative error greater than 400%, and is truly identified as LOS. From the box plots of true NLOS signals, there is one signal that has a relative error greater than 300% and is identified as LOS signal by the both the classifier. Although the regression models are able to reduce the range error of the outlying signals, the reduction is not significant. We were still able to restrict the RMSE for LOS identified signals to less than 30 cm, but failed to do so for NLOS identified signals.

Classifier	Label	Data size	Total identified	True identified	RMSE of misclassification	RMSE after Regression
SVM	LOS	1884	2097	1872	40.79cm	20.65cm
	NLOS	1012	799	787	33.76cm	24.16cm
GBM	LOS	1884	2135	1868	47.05cm	28.98cm
	NLOS	1012	761	745	28.45cm	23.96cm

Table 5.3: **Scenario 1 classification accuracy**

Classifier	Label	Data size	Total identified	True identified	RMSE of misclassification	RMSE after Regression
SVM	LOS	1921	2402	1908	85.17cm	56.935cm
	NLOS	1500	1019	1006	26.55cm	36.62cm
GBM	LOS	1921	2509	1910	85.24cm	52.948cm
	NLOS	1500	912	901	30.25cm	52.714cm

Table 5.4: **Scenario 2 classification accuracy**

5.5.3 Discussions

From the RMSE plots for LOS figure 5.12a for scenario 2, we can see that *cubist* regression is able to reduce the RMSE of predicted signals by approximately 44%, the measured RMSE after regression is still greater than the RMSE of the LOS signals in the dataset. That suggests that if we use a classifier with 100% classification accuracy of LOS and NLOS signals on Dataset 1 (soft NLOS and hard NLOS belong to the same class), the LOS signals will report a lower RMSE without without using regression. This result goes against our approach of treating LOS and soft NLOS signals as the same class.

Table 5.3 and table 5.4 summarizes the performance of classifiers in scenario 1 and 2 respectively. The table shows the initial size of the robust dataset, the total number of data classified as LOS or NLOS, the number of correctly classified signals, the measured RMSE of misclassification, and the RMSE of misclassified data after cubist regression model is applied. In scenario 2, the GBM classifier classified 2509 signals as LOS, out of which 1910 (out of 1921) signals were collected from a LOS scenario. The RMSE of the misclassified signals was 85.24 cm, which was reduced to 52.948 cm after applying regression. For LOS signals in scenario 2, the reported RMSE after regression in figure 5.12a is calculated over 2509 LOS classified signals as compared to the true LOS RMSE calculated over 1921 signals. Hence, although our classification and regression models were unable to reduce the measured RMSE lower than the RMSE of the true LOS signals, our model is able to classify 588 more signals as LOS and reduce the RMSE of the predicted signals.

Another interesting observation is the contribution of the misclassified signals by both classifiers in both scenarios. This is an indication on how well can the cubist regression model back up misclassification by the classifier. In scenario 1, we can see that the regression model is able to reduce the overall RMSE of misclassified signals for LOS and NLOS classified signals. However, in scenario 2, we see an increase in the RMSE after applying cubist regression on misclassified NLOS signals.

Chapter 6

Conclusion and Future Work

6.1 Summary

In this thesis, we evaluated the classification accuracy for LOS and NLOS signals when features from more than one antenna are used to train the model and then applied regression models to reduce the ranging error. We investigated the performance of 5 classification models (support vector machine, random forest, decision tree, gradient boosting and adaboost) using features that have been frequently used in the literature to train the model. We compared different models based on the classification accuracy, model size and the complexity of deriving the input features.

We used regression models were used to predict the true range for signals classified as LOS and as NLOS. We trained and tested regression models (random forest, gradient boosting and cubist regression) using features extracted from one and two antennas. We compared the 3 regression models based on the ranging error of the predicted range and the model size.

We evaluated the robustness of the classification and regression models after collecting LOS and NLOS data when the vehicle was parked in two parking configurations. We were able to show the improvement in ranging accuracy after classifying the signals as LOS or NLOS using SVM and gradient boost models, and then applying cubist regression for either sets of signals.

6.2 Research Questions

RQ1: *What is the impact of a second antenna on identifying NLOS signals using machine learning based classifiers?*
With the help of binary hypothesis test, we were able to show the improvement in classification of LOS and NLOS signals by some of the features that have been frequently used in the literature when they are extracted from two antennas. We further showed the improvement in classification accuracy on some of the state-of-the-art solutions when features from two antennas are used as inputs to the classification model (figure 5.7).

RQ2: *How can machine learning based regression methods be used to improve the accuracy of ranging? What is the impact on ranging accuracy when two antennas are used?*
Rf regression, *gbm regression* and *cubist regression* models were able to reduce the ranging error by approximately 79.8% in a NLOS scenario, and by 42% in a LOS scenario. For all three models, regression models that used inputs from two antennas reported a lower ranging than when features from a single antenna was used to train the model.

6.3 Discussions

As discussed in the thesis, features from the second antenna helped better identify NLOS signals, as well as reduce the measured error in LOS and NLOS scenario. From the regression models, the use of features from the second antenna did not result in a significant reduction in ranging error. Although we were able to reduce the ranging error for LOS identified signals below 30cm, we observed a large reduction in the range errors after applying regression to NLOS signals, but was unable to restrict the error to less than 30cm. This may be due to the absence of relation between the input features to the regression model and the predicted range.

6.4 Future Work

In this thesis, we used some of the channel estimation parameters as inputs to different regression models to predict the true range. Since distance measurements use the timestamps to measure the distance between two devices, it would be interesting to explore if it is possible to extract features from the timestamps measured that can be used as inputs to regression models to obtain lower ranging error.

All our experiments were conducted based on data accumulated on the anchor. One possible direction to improve the classification accuracy is by using features extracted by the tag. When the tag receives a signal, it can measure the channel parameters and send it across to the anchor, allowing the anchor to model a system where the perspective of the channel is given by both devices involved.

Bibliography

[1] S. Aditya, A. F. Molisch, and H. M. Behairy. A survey on the impact of multipath on wideband time-of-arrival based localization. *Proceedings of the IEEE*, 106(7):1183–1203, 2018.

[2] Constantine A. Balanis. Polarization. In *Antenna Theory: analysis and design*. John Wiley and Sons Ltd, 1996.

[3] V. Barral, C. J. Escudero, and J. A. Garca-Naya. Nlos classification based on rss and ranging statistics obtained from low-cost uwb devices. In *2019 27th European Signal Processing Conference (EUSIPCO)*, pages 1–5, 2019.

[4] Leo Breiman. Random forests. *Machine Learning*, 45(1):5–32, Oct 2001.

[5] F. Carpi, L. Davoli, M. Martal, A. Cilfone, Y. Yu, Y. Wang, and G. Ferrari. Rssi-based methods for los/nlos channel identification in indoor scenarios. In *2019 16th International Symposium on Wireless Communication Systems (ISWCS)*, pages 171–175, 2019.

[6] Corinna Cortes and Vladimir Vapnik. Support-vector networks. *Machine Learning*, 20(3):273–297, Sep 1995.

[7] F. T. Dagefu, G. Verma, B. M. Sadler, R. Kozick, and K. Sarabandi. Full-wave analysis of time of arrival based localization with polarization diversity. In *2017 USNC-URSI Radio Science Meeting (Joint with AP-S Symposium)*, pages 5–6, 2017.

[8] Decawave. The implementation of twoway ranging with the dw1000. `https://www.decawave.com/wp-content/uploads/2018/10/APS013_The-Implementation-of-Two-Way-Ranging-with-the-DW1000_v2.3.pdf`, 2015. Last accessed: February. 15, 2021.

[9] I. Dotlic, A. Connell, H. Ma, J. Clancy, and M. McLaughlin. Angle of arrival estimation using decawave dw1000 integrated circuits. In *2017 14th Workshop on Positioning, Navigation and Communications (WPNC)*, pages 1–6, 2017.

[10] J. Fan and A. S. Awan. Non-line-of-sight identification based on unsupervised machine learning in ultra wideband systems. *IEEE Access*, 7:32464–32471, 2019.

[11] First report and order 02-48. Federal communications commission, Feb 2002.

[12] Yoav Freund and Robert E Schapire. A decision-theoretic generalization of on-line learning and an application to boosting. *Journal of Computer and System Sciences*, 55(1):119–139, 1997.

[13] Jerome H. Friedman. Greedy function approximation: A gradient boosting machine. *The Annals of Statistics*, 29(5):1189–1232, 2001.

[14] S. Galler, W. Gerok, J. Schroeder, Kyandoghere Kyamakya, and T. Kaiser. Combined aoa/toa uwb localization. In *2007 International Symposium on Communications and Information Technologies*, pages 1049–1053, 2007.

[15] S. Gezici and H. V. Poor. Position estimation via ultra-wide-band signals. *Proceedings of the IEEE*, 97(2):386–403, 2009.

[16] I. Guvenc and Z. Sahinoglu. Threshold-based toa estimation for impulse radio uwb systems. In *2005 IEEE International Conference on Ultra-Wideband*, pages 420–425, 2005.

[17] C. Huang, A. F. Molisch, R. He, R. Wang, P. Tang, B. Ai, and Z. Zhong. Machine learning-enabled los/nlos identification for mimo systems in dynamic environments. *IEEE Transactions on Wireless Communications*, 19(6):3643–3657, 2020.

[18] S. Jeong, T. Sung, K. E. Lee, and J. Kang. Joint toa/aoa-based localization in wireless sensor networks. In *2014 8th International Conference on Signal Processing and Communication Systems (ICSPCS)*, pages 1–5, 2014.

[19] J. B. Kristensen, M. Massanet Ginard, O. K. Jensen, and M. Shen. Non-line-of-sight identification for uwb indoor positioning systems using support vector machines. In *2019 IEEE MTT-S International Wireless Symposium (IWS)*, pages 1–3, 2019.

[20] S. Li, B. Song, and K. Luo. Nlos mitigation for uwb localization based on machine learning fusion method. In *2019 IEEE Symposium Series on Computational Intelligence (SSCI)*, pages 1048–1055, 2019.

[21] Li Cong and Weihua Zhuang. Nonline-of-sight error mitigation in mobile location. *IEEE Transactions on Wireless Communications*, 4(2):560–573, 2005.

[22] W. Q. Malik and D. J. Edwards. Uwb impulse radio with triple-polarization simo. In *IEEE GLOBECOM 2007 - IEEE Global Telecommunications Conference*, pages 4124–4128, 2007.

[23] S. Maran, W. M. Gifford, H. Wymeersch, and M. Z. Win. Nlos identification and mitigation for localization based on uwb experimental data. *IEEE Journal on Selected Areas in Communications*, 28(7):1026–1035, 2010.

[24] A. H. Muqaibel, M. A. Landolsi, and M. N. Mahmood. Practical evaluation of nlos/los parametric classification in uwb channels. In *2013 1st International Conference on Communications, Signal Processing, and their Applications (ICCSPA)*, pages 1–6, 2013.

[25] Pi-Chun Chen. A non-line-of-sight error mitigation algorithm in location estimation. In *WCNC. 1999 IEEE Wireless Communications and Networking Conference (Cat. No.99TH8466)*, volume 1, pages 316–320 vol.1, 1999.

[26] J Quinlan. Combining instance-based and model-based learning. In *In International Conference on Machine Learning (ICML), pages 236243*, 1999.

[27] L. Schmid, D. Salido-Monz, and A. Wieser. Accuracy assessment and learned error mitigation of uwb tof ranging. In *2019 International Conference on Indoor Positioning and Indoor Navigation (IPIN)*, pages 1–8, 2019.

[28] M. Sharma, C. G. Parini, and A. Alomainy. Influence of antenna alignment and line-of-sight obstruction on the accuracy of range estimates between a pair of miniature uwb antennas. In *2015 9th European Conference on Antennas and Propagation (EuCAP)*, pages 1–5, 2015.

[29] B. Silva and G. P. Hancke. Ir-uwb-based non-line-of-sight identification in harsh environments: Principles and challenges. *IEEE Transactions on Industrial Informatics*, 12(3):1188–1195, 2016.

[30] Z. Tan, X. Zhu, Z. Zhao, B. Liu, Z. Zhu, M. Li, and Z. Nie. Uwb-aoa estimation method based on a spare antenna array with virtual element. In *2018 IEEE International Conference on Computational Electromagnetics (ICCEM)*, pages 1–3, 2018.

[31] S. Umadevi and K. S. J. Marseline. A survey on data mining classification algorithms. In *2017 International Conference on Signal Processing and Communication (ICSPC)*, pages 264–268, 2017.

[32] Weijie Li, Tingting Zhang, and Qinyu Zhang. Experimental researches on an uwb nlos identification method based on machine learning. In *2013 15th IEEE International Conference on Communication Technology*, pages 473–477, 2013.

[33] B. You, X. Li, X. Zhao, and Y. Gao. A novel robust algorithm attenuating non-line-of-sight errors in indoor localization. In *2015 IEEE International Conference on Communication Software and Networks (ICCSN)*, pages 6–11, 2015.

[34] R. Zandian and U. Witkowski. Differential nlos error detection in uwb-based localization systems using logistic regression. In *2018 15th Workshop on Positioning, Navigation and Communications (WPNC)*, pages 1–6, 2018.

[35] Z. Zeng, S. Liu, and L. Wang. Nlos identification for uwb based on channel impulse response. In *2018 12th International Conference on Signal Processing and Communication Systems (ICSPCS)*, pages 1–6, 2018.

[36] J. Zhang, J. Salmi, and E. Lohan. Analysis of kurtosis-based los/nlos identification using indoor mimo channel measurement. *IEEE Transactions on Vehicular Technology*, 62(6):2871–2874, 2013.